

2015年7月10日

素粒子宇宙論研究室セミナー

@神戸大学

Perturbation theory approach to large-scale structure formation

~ Success, limitation & beyond ~

樽家 篤史
(京大基研)

内容

宇宙大規模構造の理論的取り扱いをめぐる最近の進展と課題

宇宙大規模構造と精密宇宙論

宇宙大規模構造の理論的記述

(N体シミュレーション)

摂動論的アプローチとその問題点

有効理論？

In collaboration with

F. Bernardeau, S. Codis, T. Hiramatsu, T. Nishimichi, S. Saito, ...

宇宙大規模構造

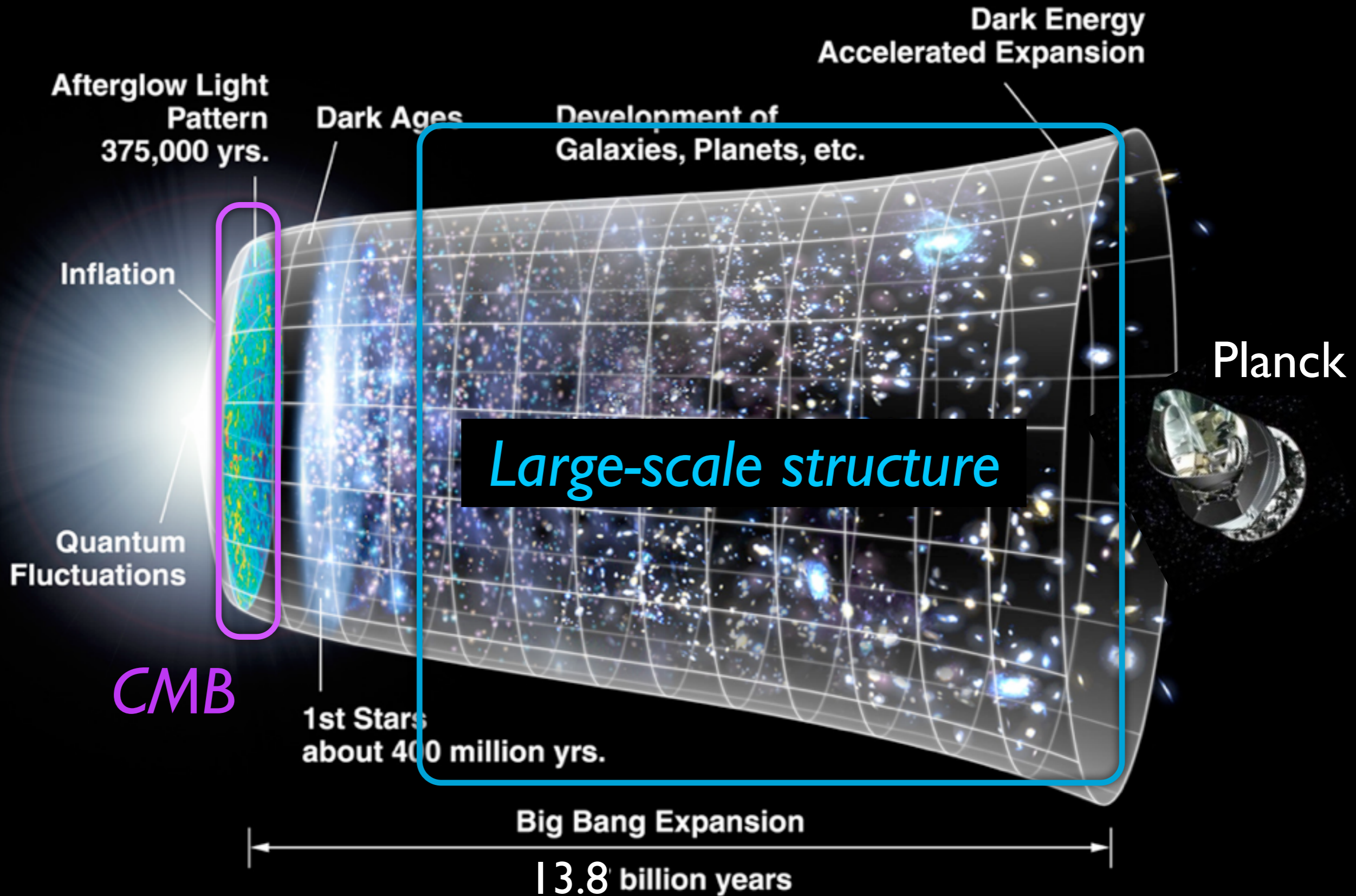
Large-scale structure of the Universe

銀河の3次元分布に反映される、
大スケールにわたる質量分布の非一様な空間パターン

- 冷たい暗黒物質 (+バリオン) の質量分布を反映
- 原始密度ゆらぎを種として、重力不安定性によって
構造が進化・発達

重力が支配する日常から遠くかけ離れた物理系

Time line of the Universe

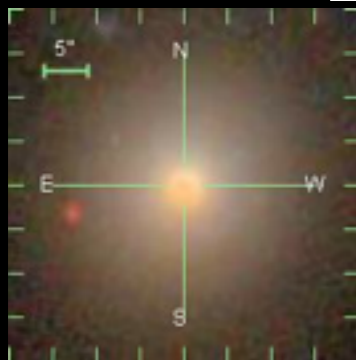


銀河赤方偏移サーベイ

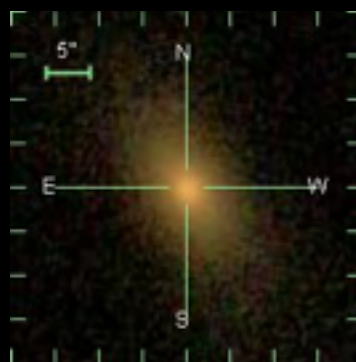
(宇宙大規模構造の代表的観測手法)

銀河1つ1つを分光観測して赤方偏移を決定、
銀河分布の3次元地図を作成

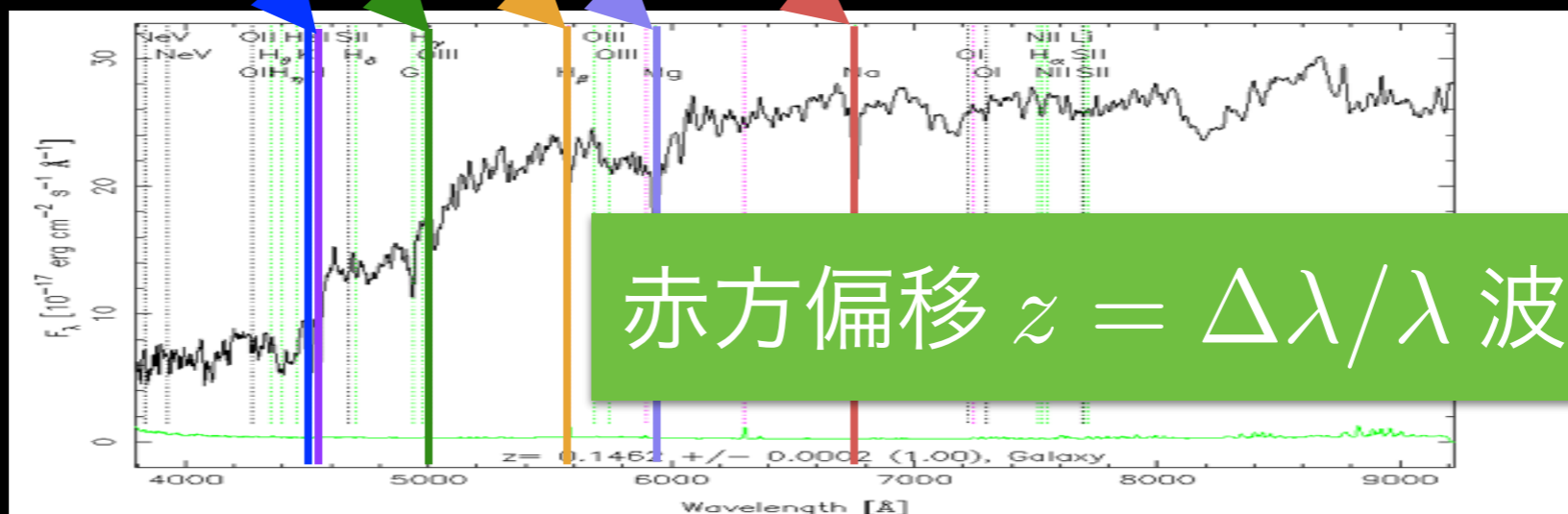
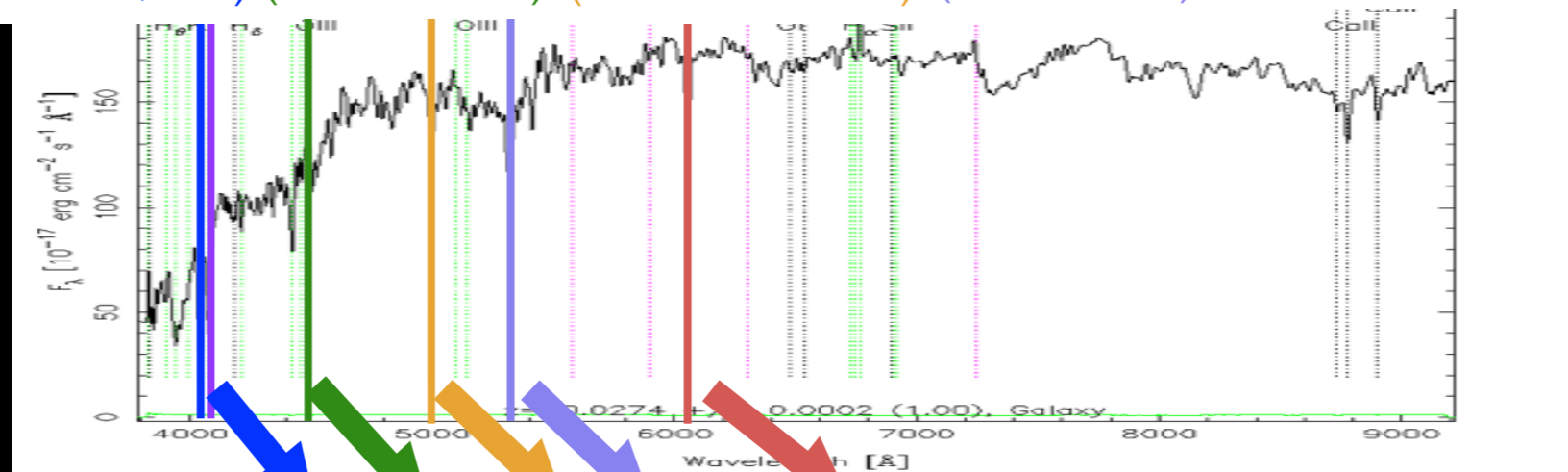
Ca H & K (カルシウムH, K線) OIII (酸素2階電離) H β (水素バルマー線) Na (ナトリウム) Mg (マグネシウム)



近傍



遠方

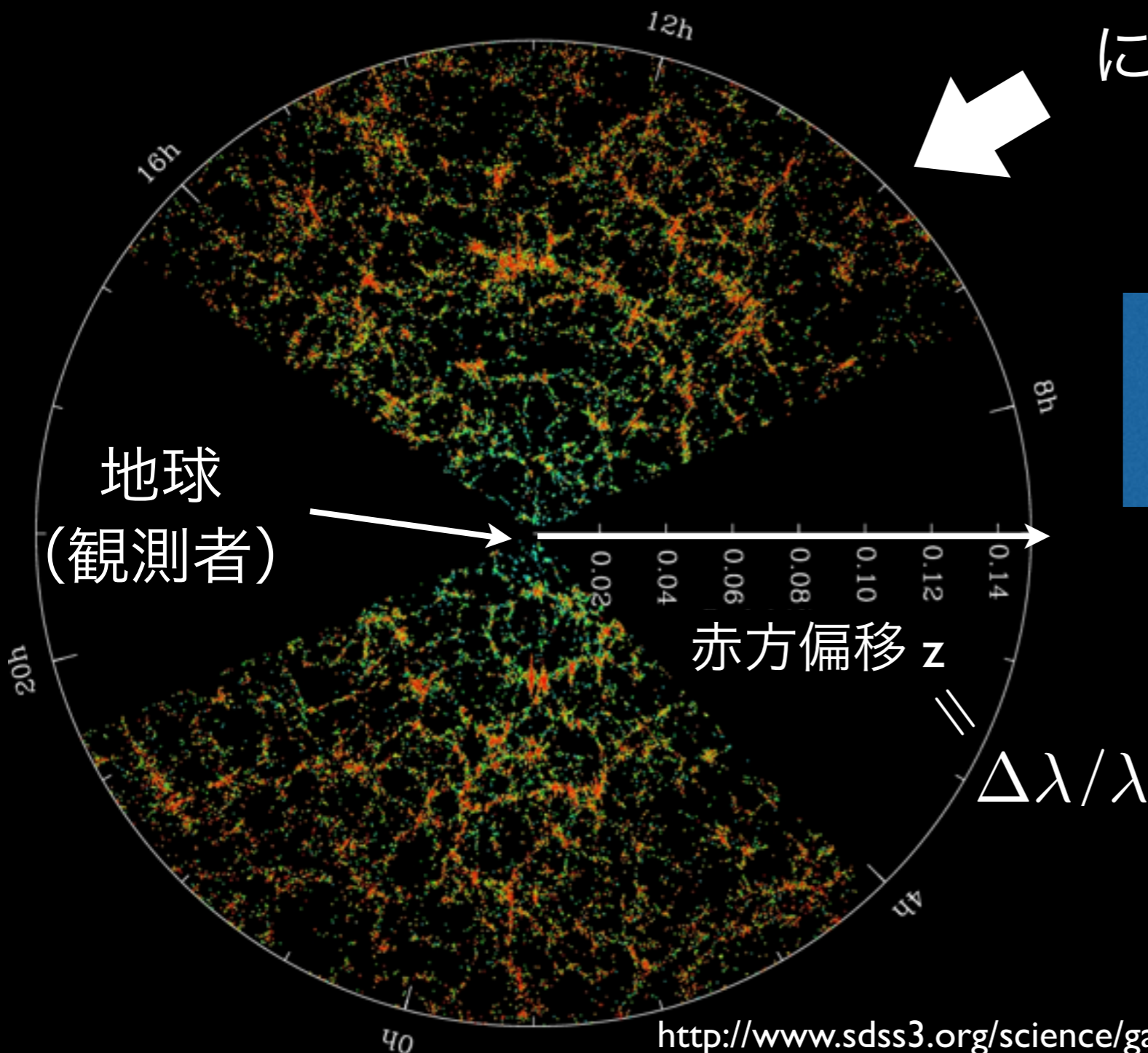


赤方偏移 $z = \Delta\lambda/\lambda$ 波長のずれ

SDSS
SkyServer

赤方偏移銀河カタログ

スローンデジタルスカイサーベイII
による赤方偏移銀河カタログ
(角度2.5度のスライス)



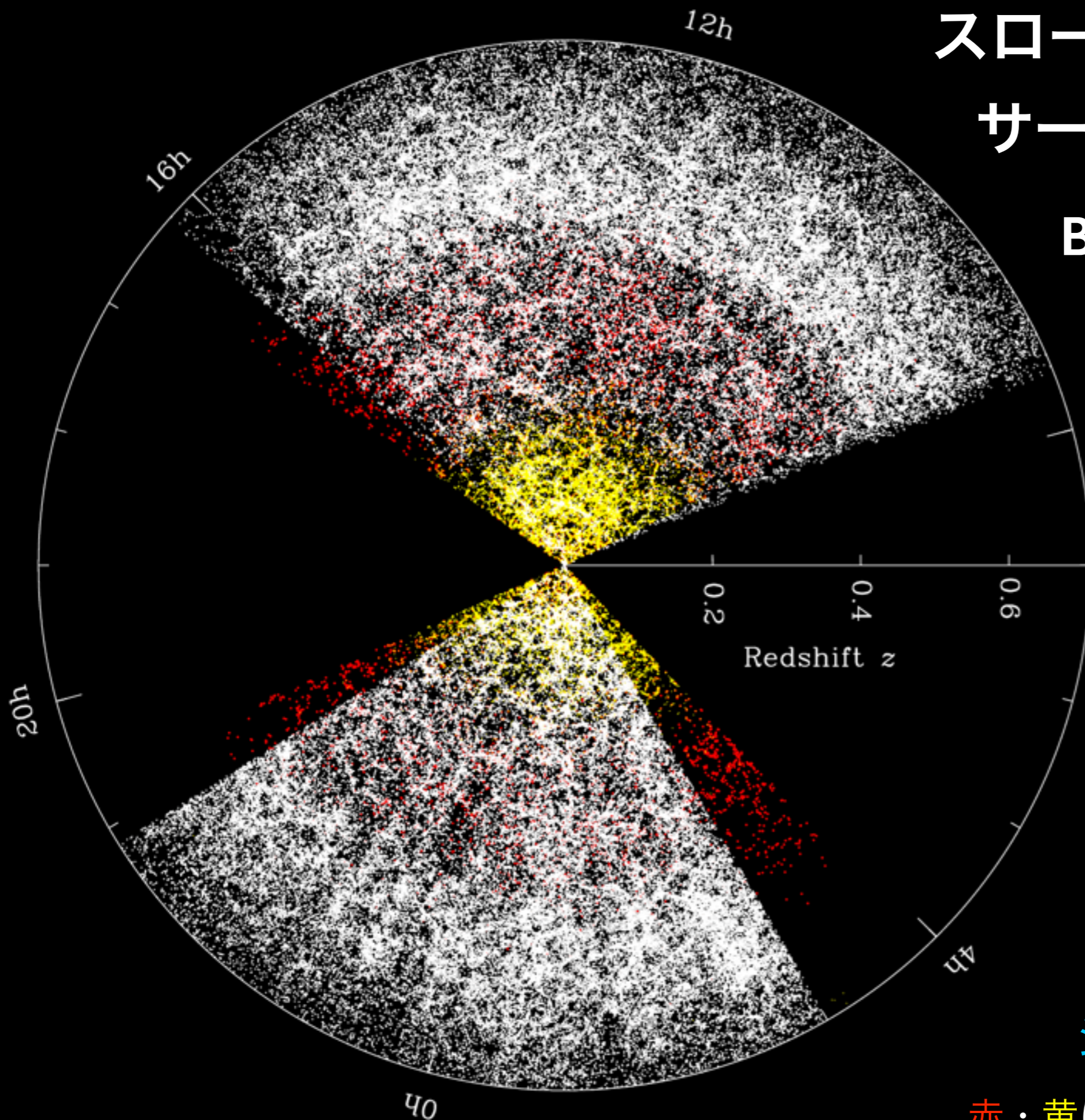
巨大な空間パターン
= 宇宙大規模構造

色は銀河の年齢

青い：若い
赤い：古い

スローンデジタルスカイ サーベイIII (SDSS III)

BOSS による銀河と クェーサーの地図 (2011年現在)



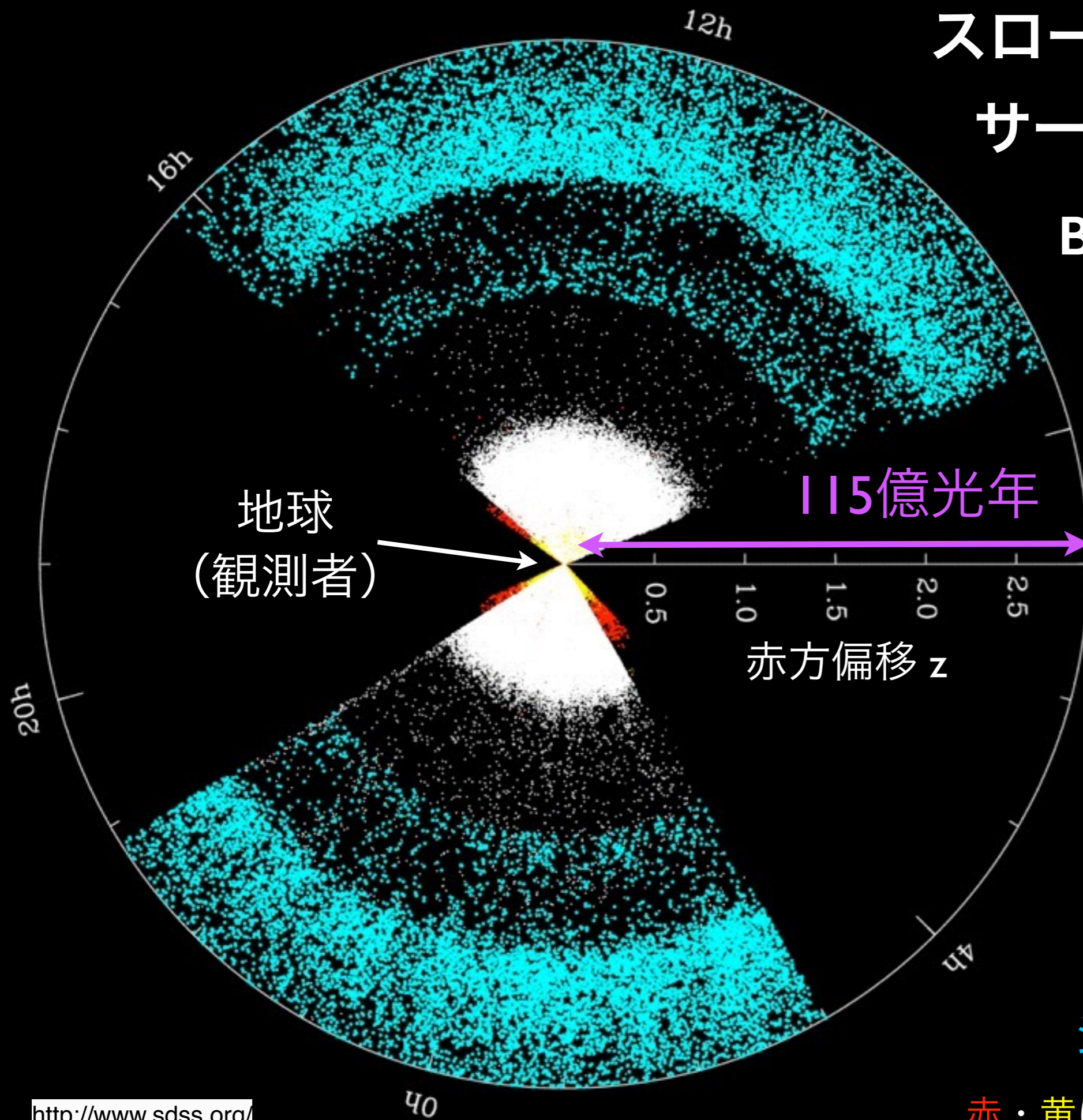
白：銀河

シアン：クェーサー

赤・黄はSDSS I / IIで観測された銀河

スローンデジタルスカイ サーベイIII (SDSS III)

BOSS による銀河と クェーサーの地図 (2011年現在)



白：銀河

シアン：クェーサー

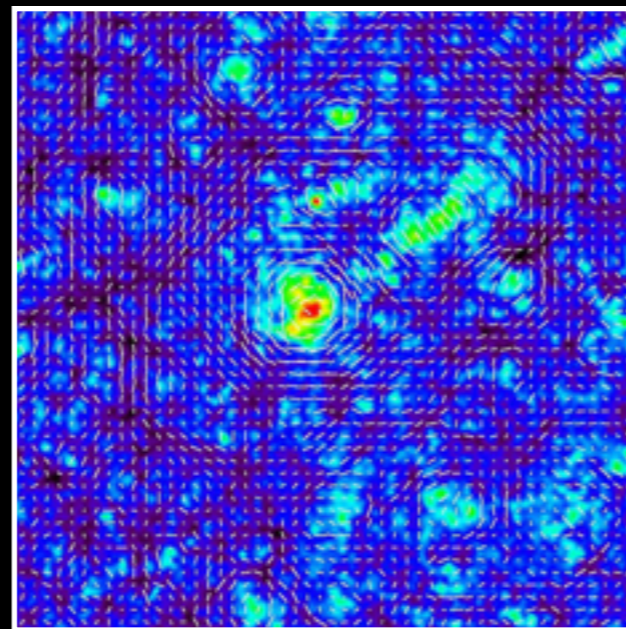
赤・黄はSDSS I / IIで観測された銀河

他の宇宙大規模構造観測

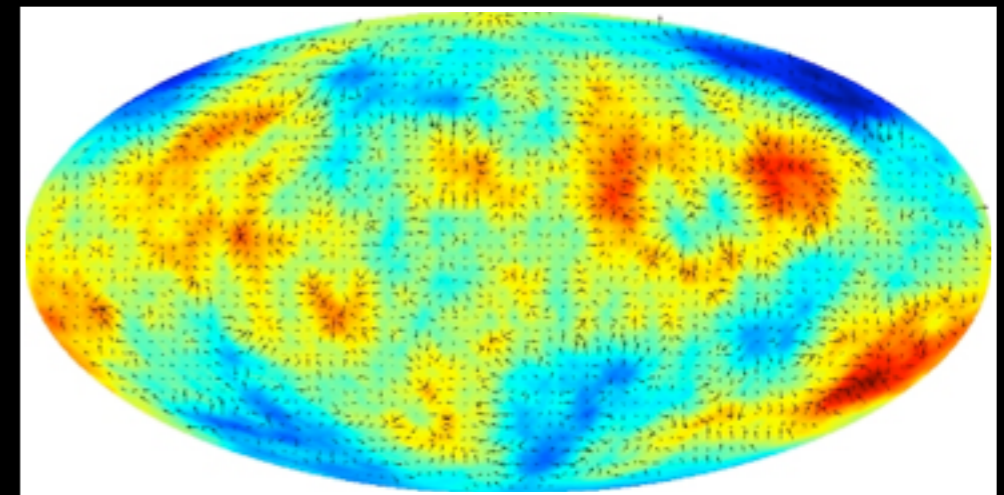
重力レンズ効果を用いて天球面に射影された

ダークマターの質量分布をプローブ

コスミックシア

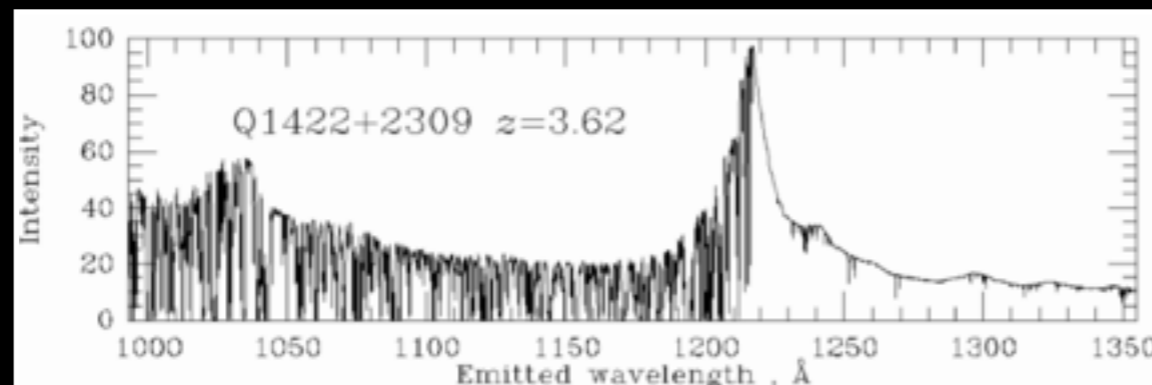


CMB レンズング



背景天体のスペクトルを通してバリオンの質量分布をプローブ

ライマンアルファの森

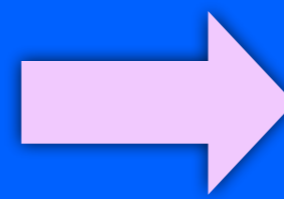


21cm 線 (将来)

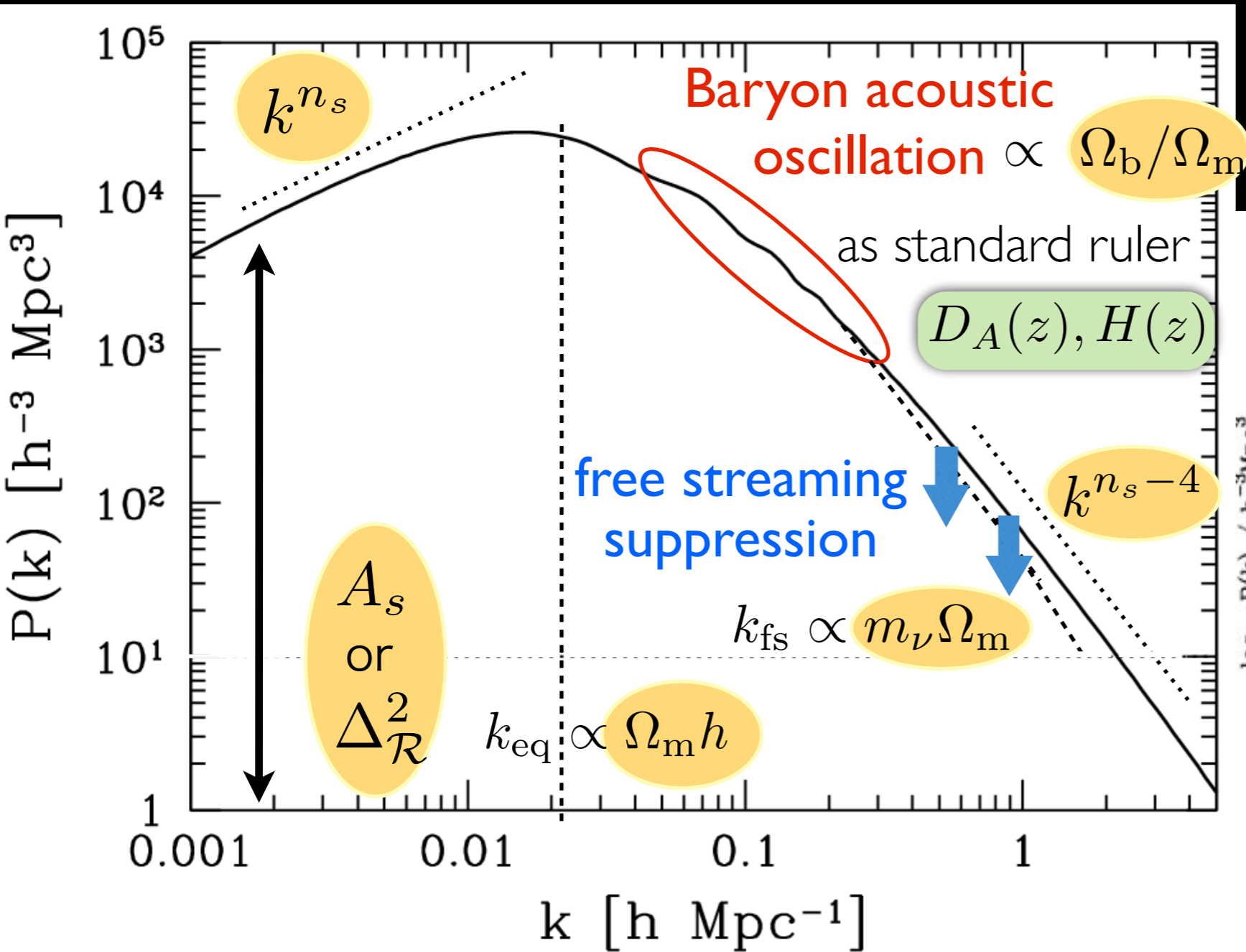


宇宙論的情報

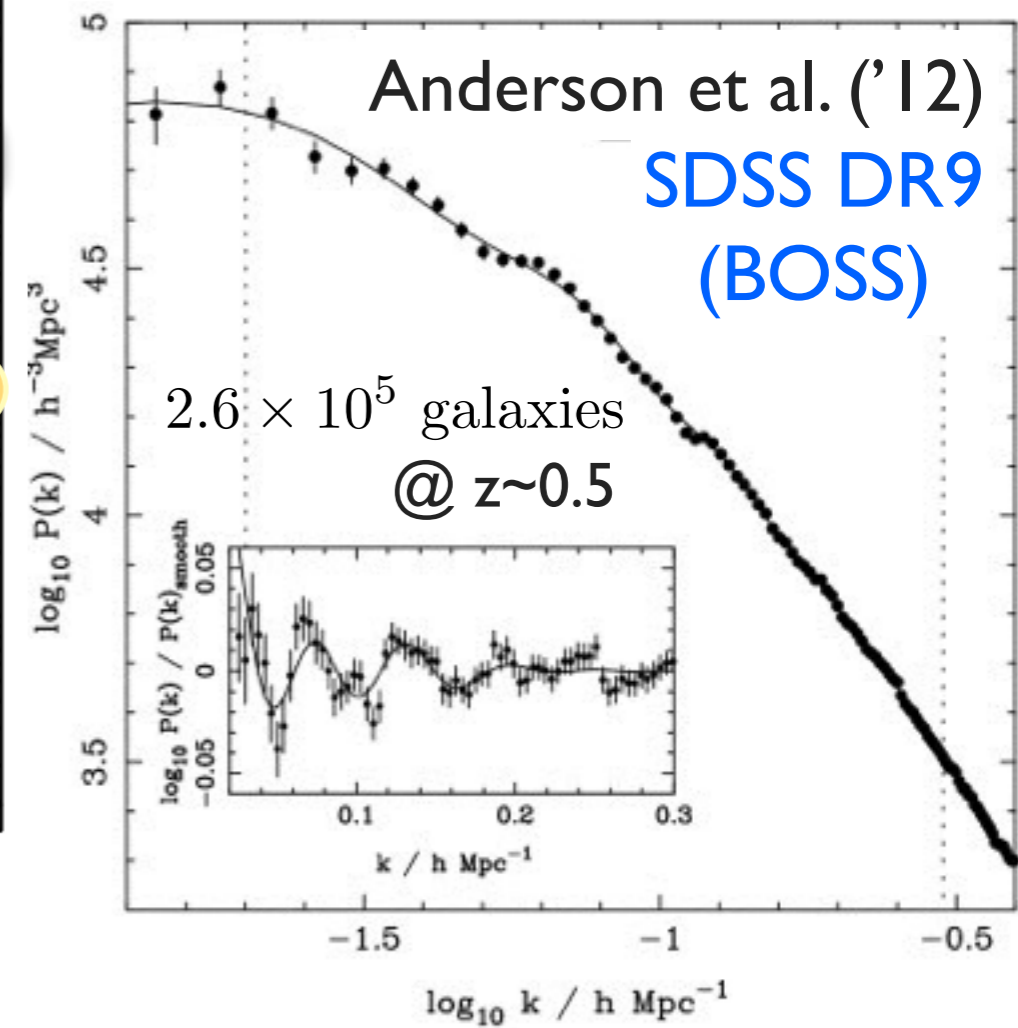
$$\delta(\vec{x}) \equiv \frac{\delta\rho_m(\vec{x})}{\bar{\rho}_m} = \frac{1}{\sqrt{V}} \sum_{\vec{k}} \delta(\vec{k}) e^{i\vec{k}\cdot\vec{x}}$$



$$P(k) = \frac{1}{N_k} \sum_{|\vec{k}|=k} |\delta(\vec{k})|^2$$



パワースペクトル

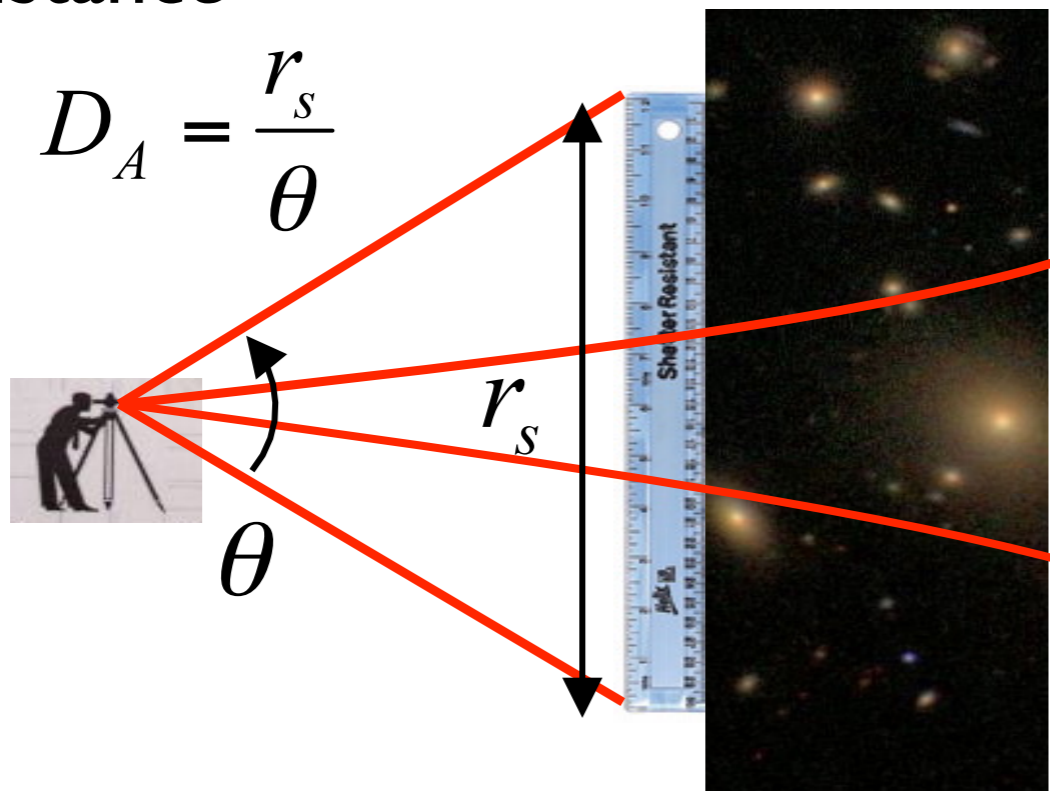


バリオン音響振動 (BAO)

- 宇宙大規模構造に刻まれたバリオン・光子流体の音響振動パターン (~150Mpc) (⇔ CMB 音響シグナル)
- 標準ものさしとして、遠方銀河分布までの距離測定に使用

Angular diameter distance

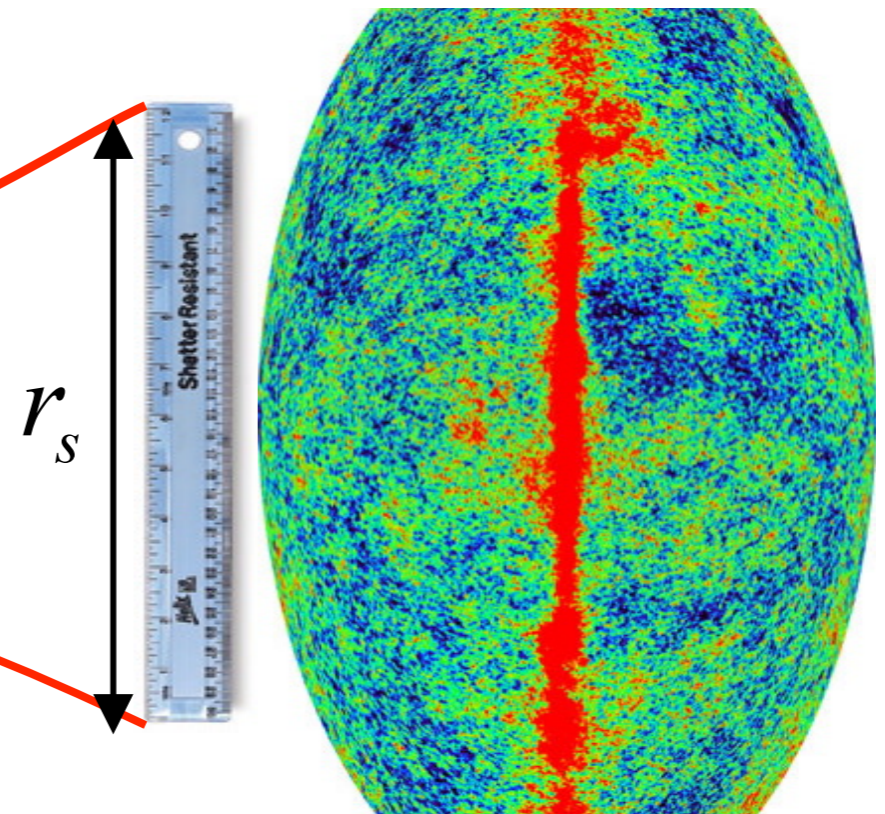
$$D_A = \frac{r_s}{\theta}$$



distant galaxies

Redshift z ($=0\sim3$)

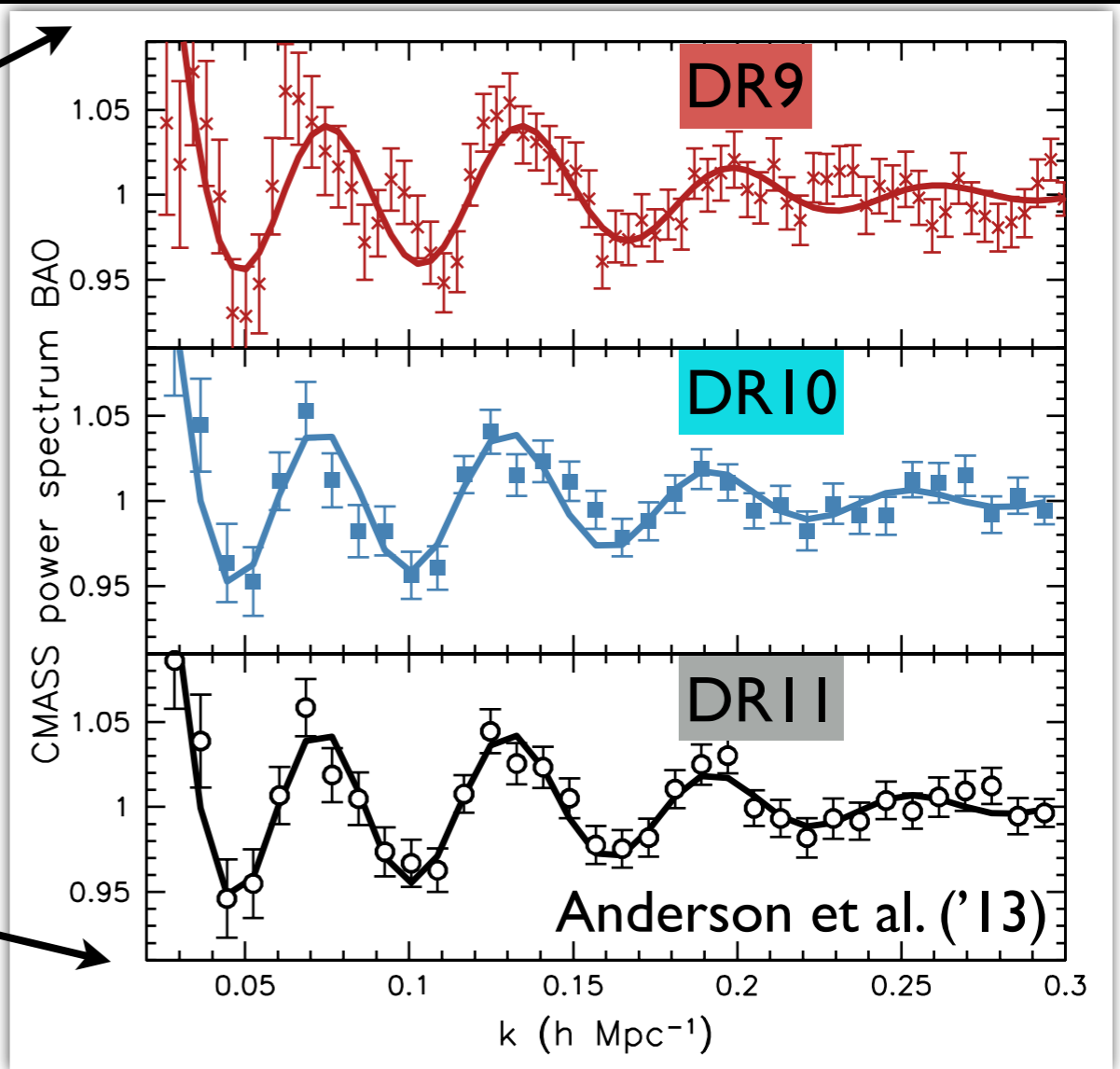
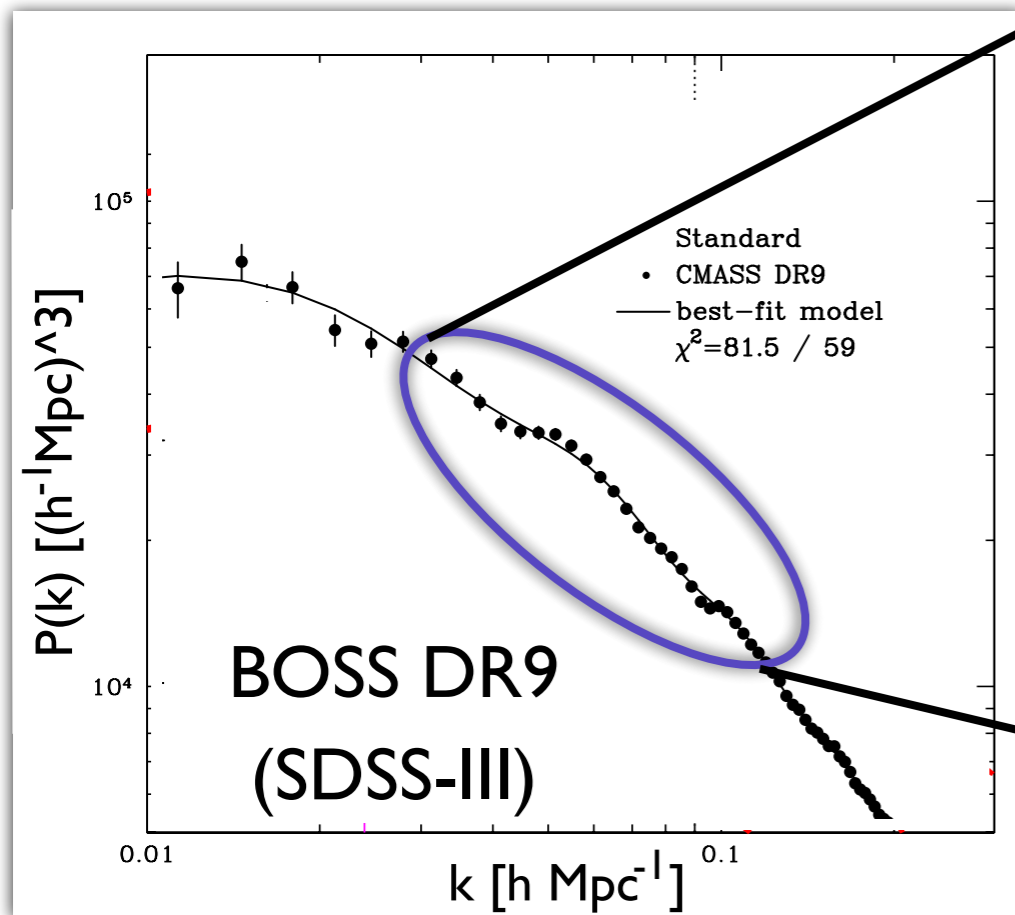
Redshift $z=1100$



cosmic microwave background

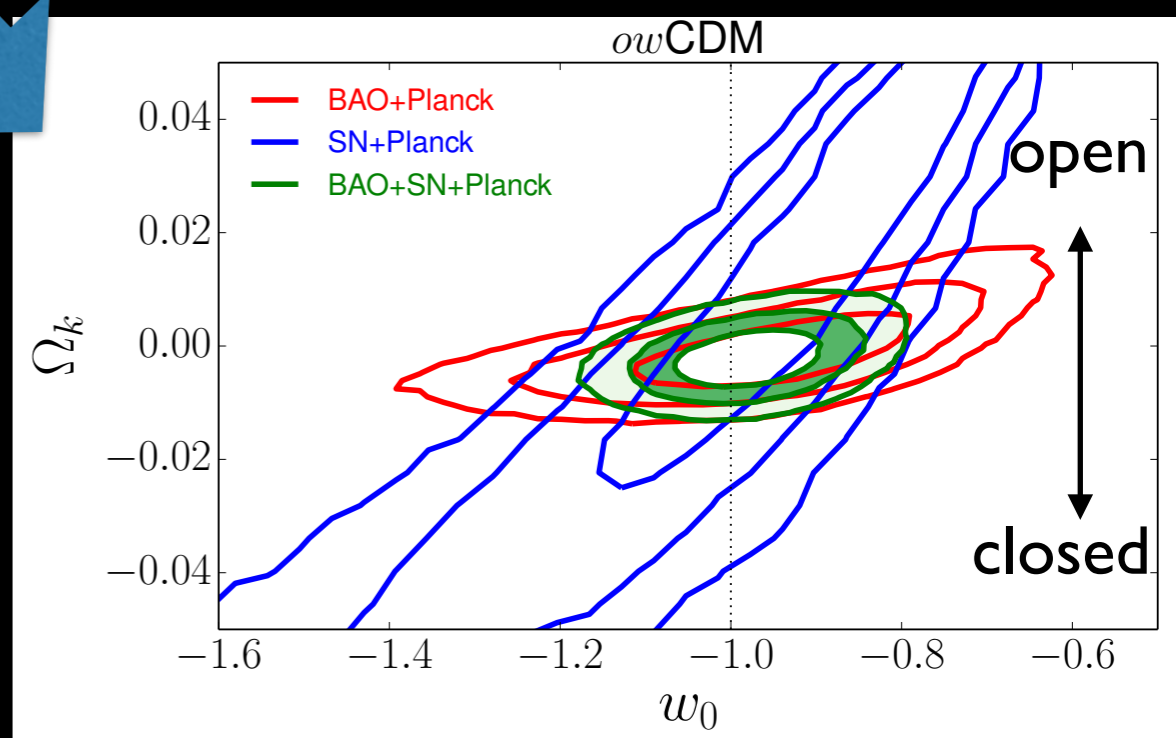
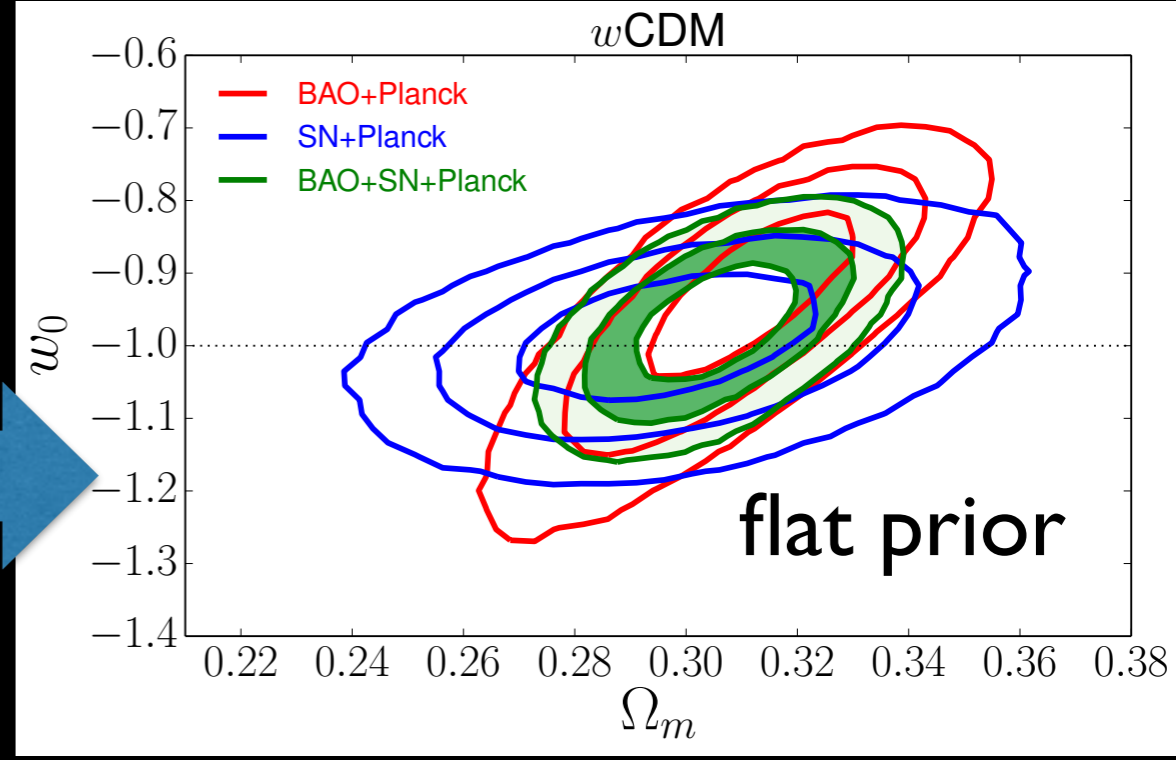
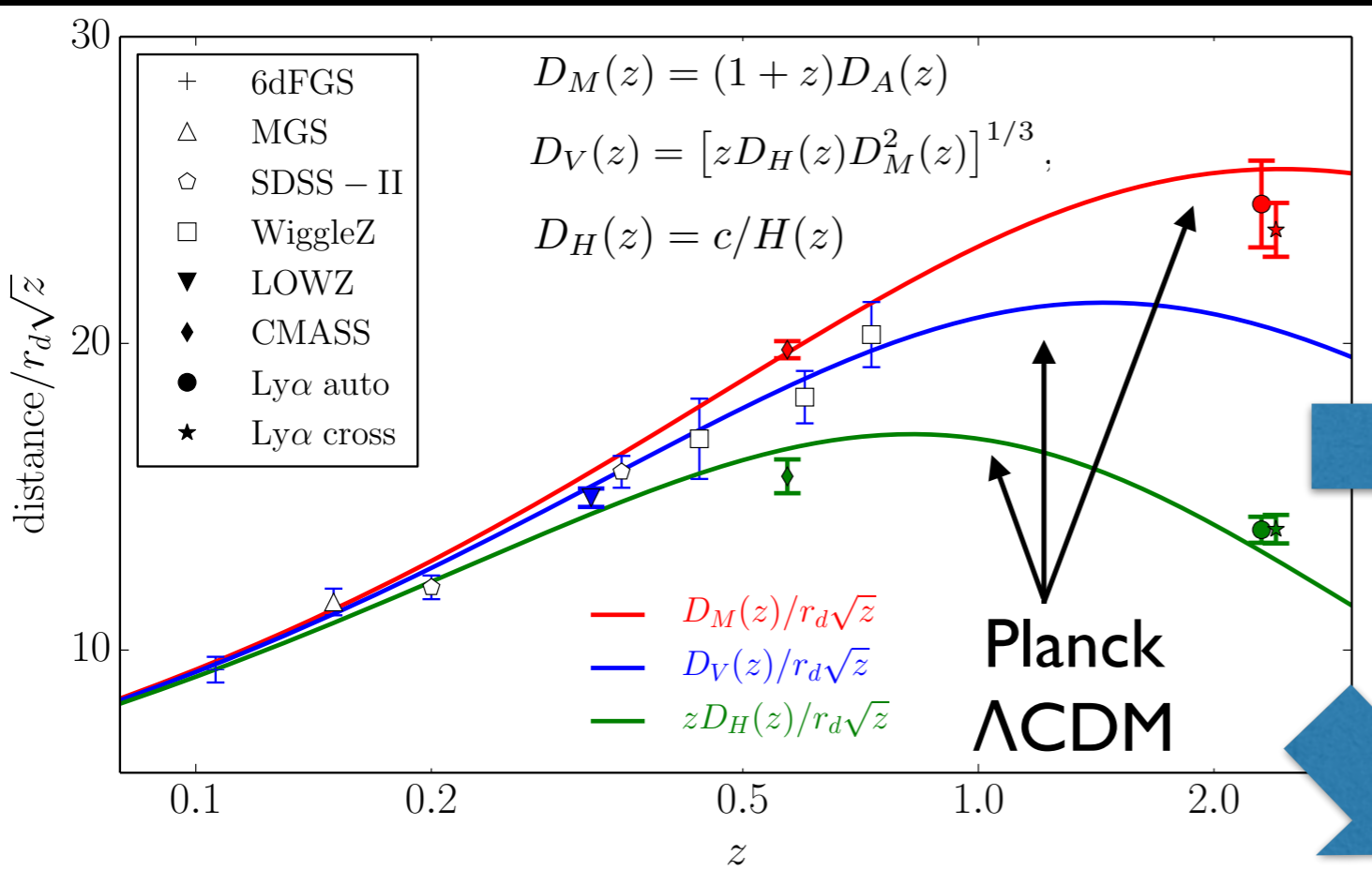
バリオン音響振動 (BAO)

- 宇宙大規模構造に刻まれたバリオン・光子流体の音響振動パターン ($\sim 150\text{Mpc}$) (\Leftrightarrow CMB 音響シグナル)
- 標準ものさしとして、遠方銀河分布までの距離測定に使用



BAO観測による宇宙論的制限

Aubourg et al. ('14)



Ω_m : 質量密度パラメーター
 Ω_k : 曲率パラメーター
 w_0 : ダークエネルギーの状態方程式
 パラメーター(宇宙定数なら -1)

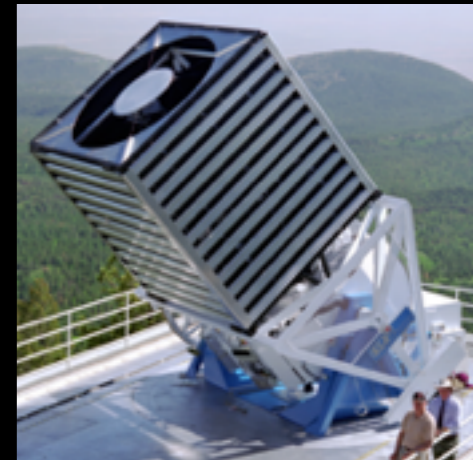
World-wide competition

Primary science goal is to clarify the nature of dark energy



BOSS
(~2014)

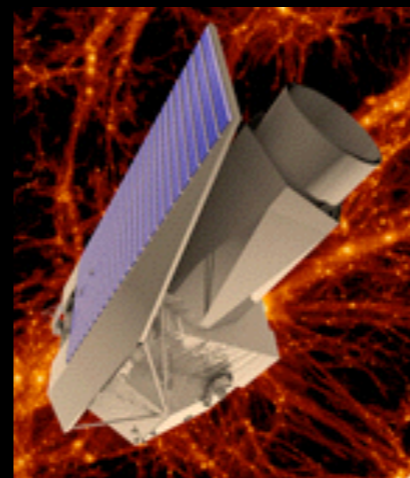
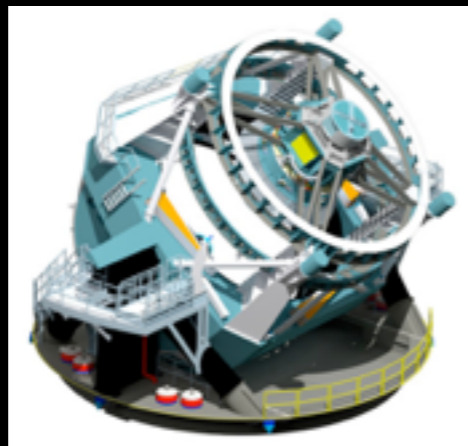
eBOSS
(2014~)



DESI
(2018+)



LSST (2022+)



WFIRST
(2024+)

EUCLID
(2020)



すばる望遠鏡による宇宙論観測



FastSound (2012~2014)

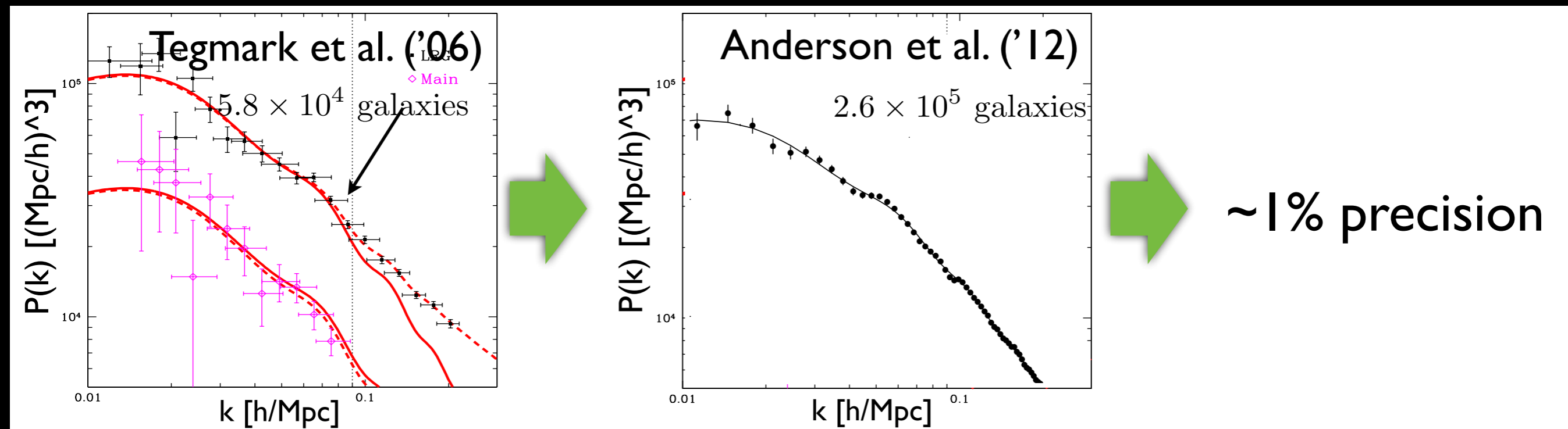
SuMIRe
(2014~)

Hyper-Suprime Cam
Prime Focus Spectrograph



精密宇宙論における不安

大規模観測により観測データの統計精度は飛躍的に向上



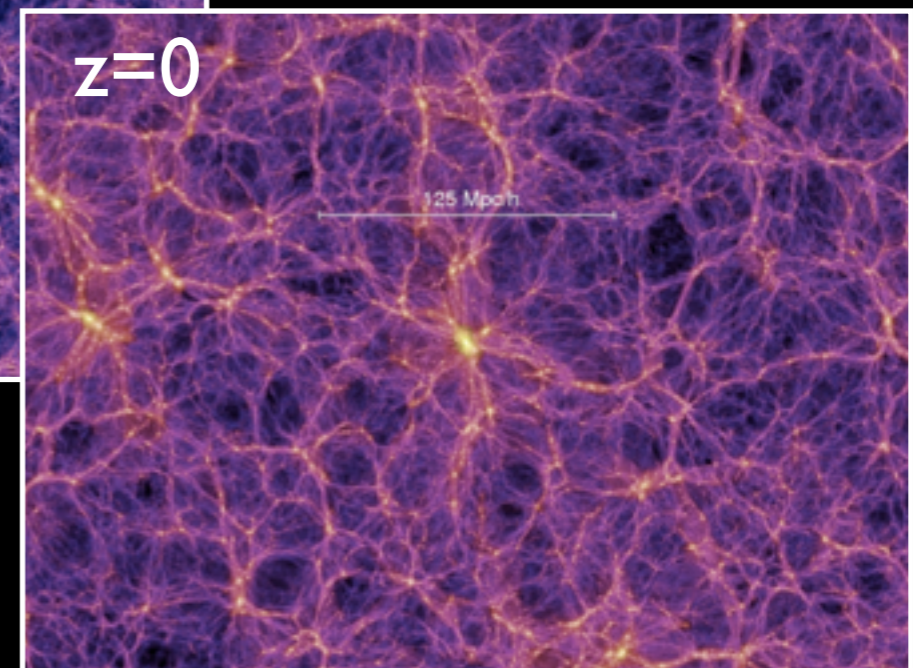
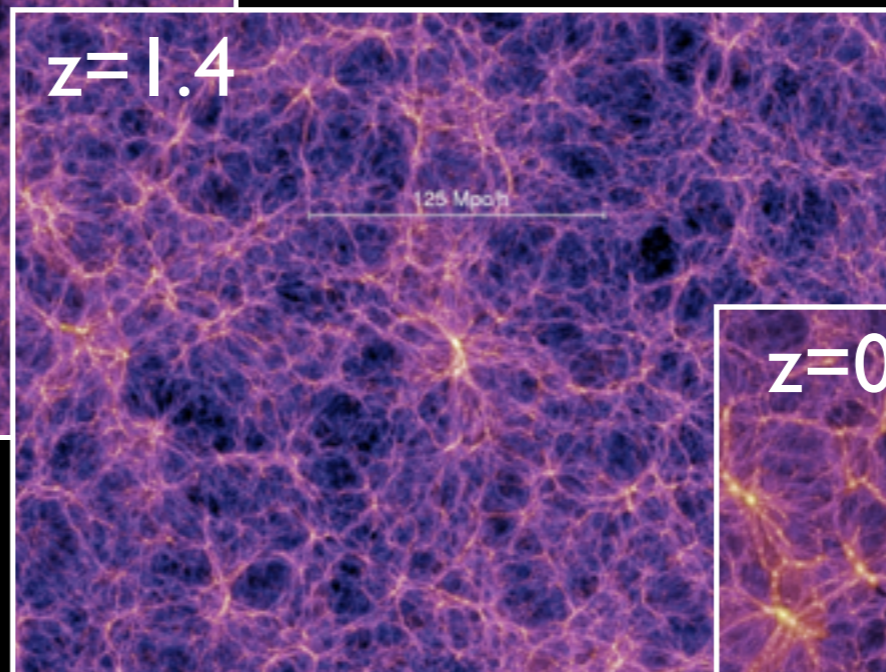
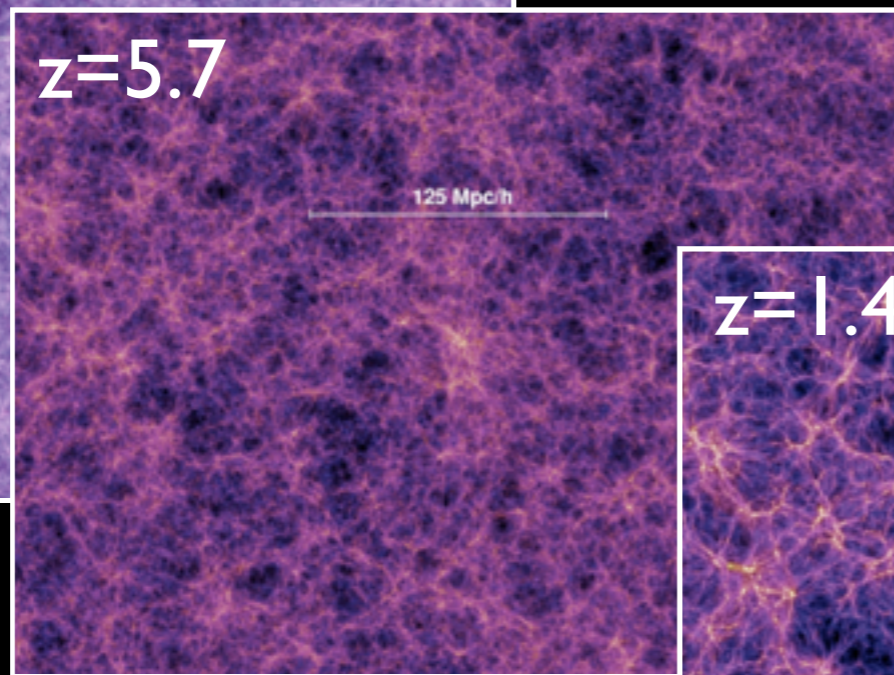
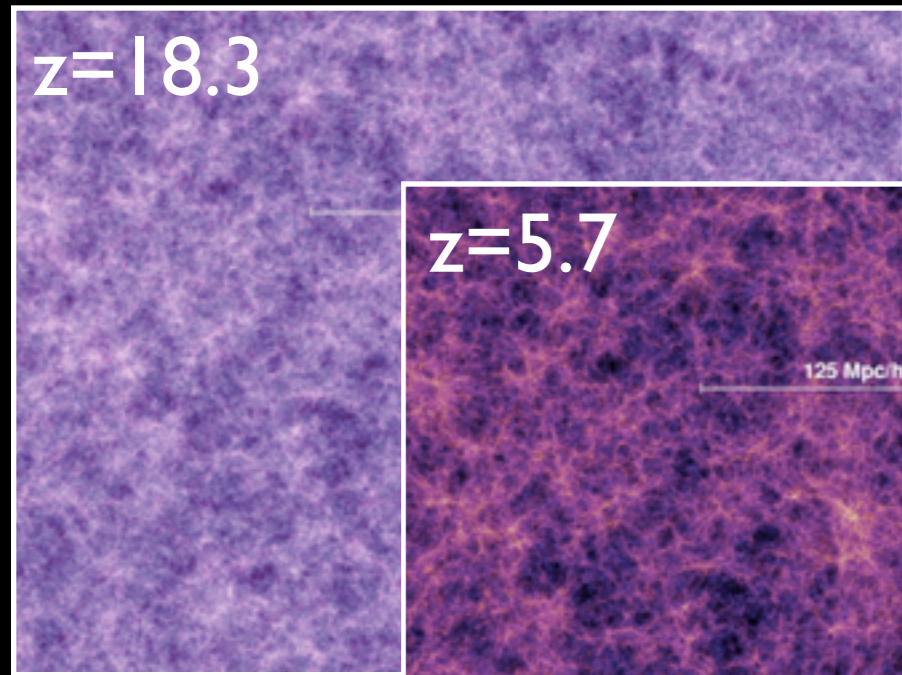
質のよい統計データで新しい宇宙研究が拓ける可能性
一方、

系統誤差が結論に影響を与える可能性

→ 観測と理論を比較する際、考慮すべき
(その影響を理論に取り込むべき)

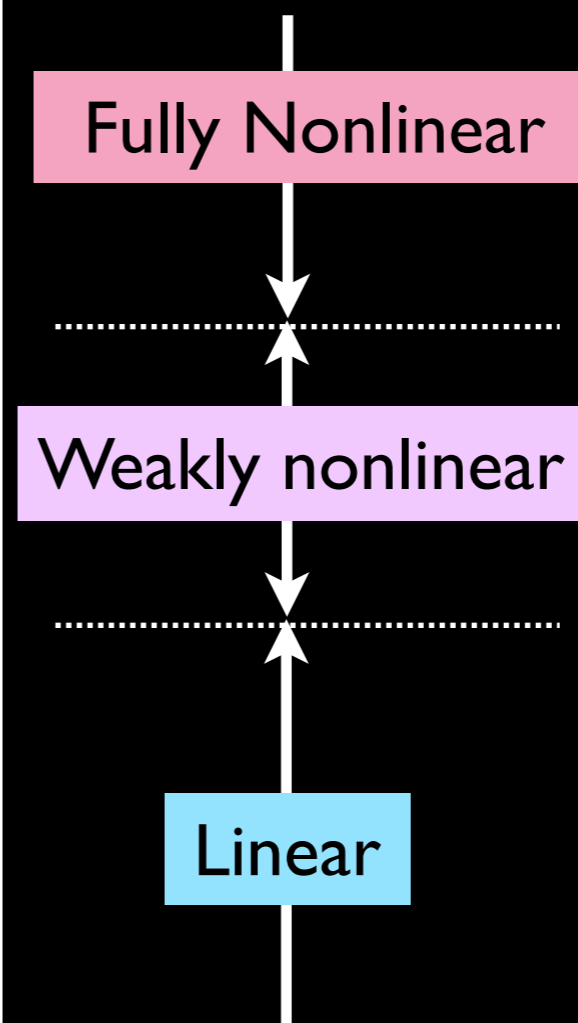
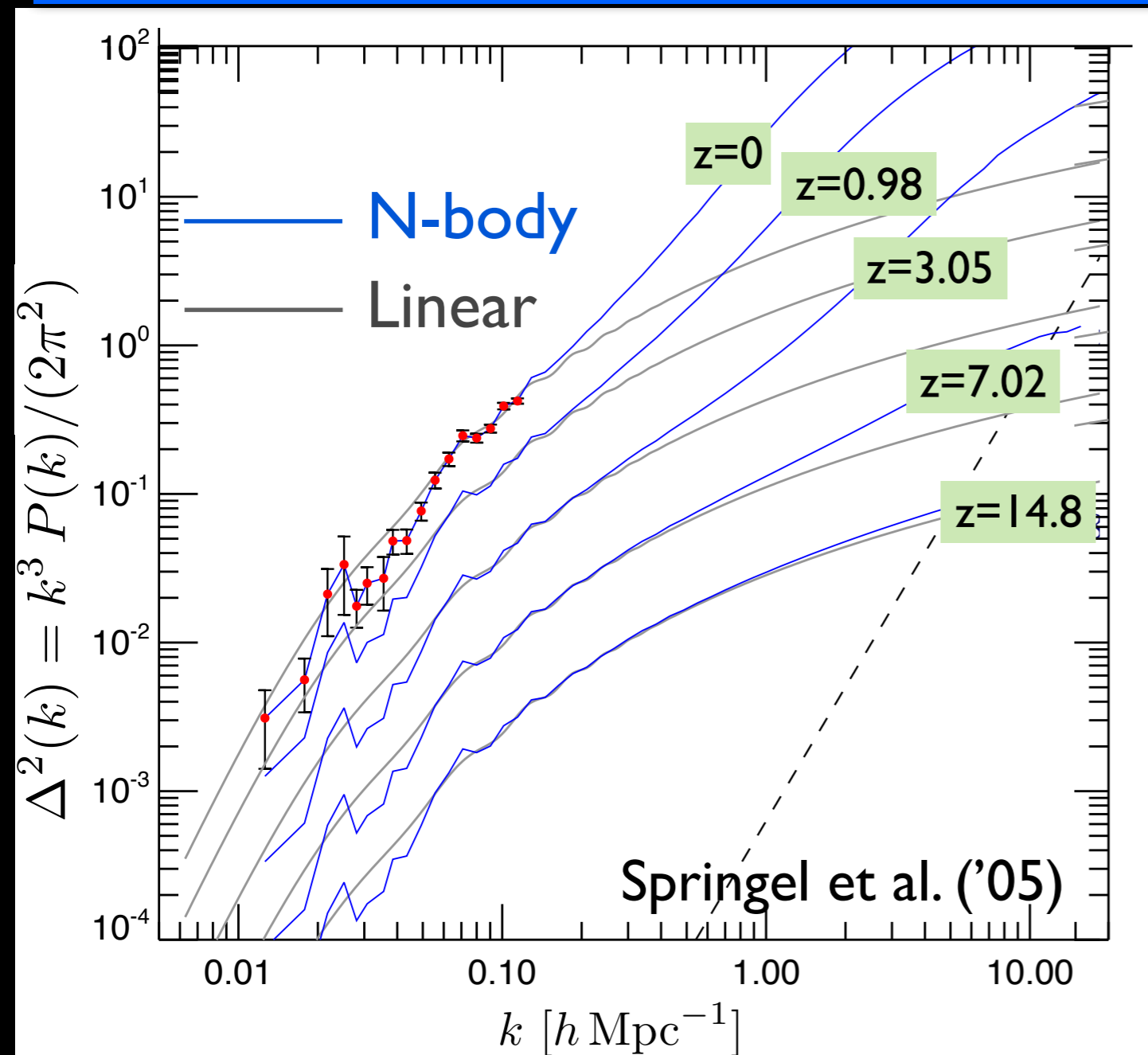
Late-time gravitational evolution

Nonlinear matter clustering
driven by gravitational interaction



パワースペクトルの非線形進化

$$\delta(\vec{x}) \equiv \frac{\delta\rho_m(\vec{x})}{\bar{\rho}_m} = \frac{1}{\sqrt{V}} \sum_{\vec{k}} \delta(\vec{k}) e^{i\vec{k}\cdot\vec{x}} \quad \longrightarrow \quad P(k) = \frac{1}{N_k} \sum_{|\vec{k}|=k} |\delta(\vec{k})|^2$$



こうした影響をどこまで
正確に取り扱えるか？

主な解析手法と適用範囲

$$\Delta^2(k) \equiv \frac{k^3 P(k)}{2\pi^2}$$

Methods (Gravitational evolution)

Other systematics

Fully nonlinear
($\Delta^2 > 1$)

N-body simulation

most powerful, but extensive
& time-consuming

(c.f. fitting formula)

weakly nonlinear
($\Delta^2 \lesssim 1$)

Perturbation theory

limited range of application, but
analytical & very fast

linear
($\Delta^2 \ll 1$)

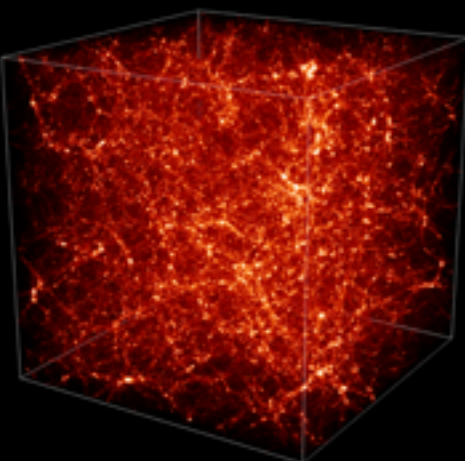
Linear theory
(CMB Boltzmann code)

very difficult

Baryon physics
(weak lensing)

- Galaxy bias
- Redshift-space distortion
(galaxy surveys)

relatively easy



N-body simulation

cold dark matter + baryon = self-gravitating many-body system
(with periodic boundary condition)

$N \rightarrow \infty$

$$\frac{\vec{p}_i}{dt} = -\frac{Gm^2}{a} \sum_{j \neq i}^N \frac{\vec{x}_i - \vec{x}_j}{|\vec{x}_i - \vec{x}_j|^3} \quad \vec{p}_i = ma^2 \frac{d\vec{x}_i}{dt} \quad (i = 1, 2, \dots, N)$$

- 無衝突系になるよう粒子数は十分大きく取る (e.g., $N \sim 1024^3$)
 → ツリー法もしくは PM法による力の(近似)計算
- 観測に合わせて計算ボックスは十分大きく取る ($L \sim 1 \text{ Gpc}/h$)
- 統計解析のためシミュレーションの試行回数も大きく取る
(> 10 realizations)

Perturbation theory (PT)

Cold dark matter + baryons = pressureless & irrotational fluid

Juszkiewicz ('81), Vishniac ('83), Goroff et al. ('86), Suto & Sasaki ('91), Makino, Sasaki & Suto ('92), Jain & Bertschinger ('94), ...

Basic
eqs.

$$\frac{\partial \delta}{\partial t} + \frac{1}{a} \vec{\nabla} \cdot [(1 + \delta) \vec{v}] = 0$$

$$\frac{\partial \vec{v}}{\partial t} + \frac{\dot{a}}{a} \vec{v} + \frac{1}{a} (\vec{v} \cdot \vec{\nabla}) \vec{v} = -\frac{1}{a} \vec{\nabla} \Phi$$

$$\frac{1}{a^2} \nabla^2 \Phi = 4\pi G \bar{\rho}_m \delta$$

*Single-stream approx. of
collisionless Boltzmann eq.*

(→ validity of this approx.?)

standard PT

$$|\delta| \ll 1$$

$$\delta = \delta^{(1)} + \delta^{(2)} + \delta^{(3)} + \dots \quad \langle \delta(\mathbf{k}; t) \delta(\mathbf{k}'; t) \rangle = (2\pi)^3 \delta_D(\mathbf{k} + \mathbf{k}') P(|\mathbf{k}|; t)$$

A more on PT calculation

In Fourier space,

$$H^{-1} \frac{\partial \delta(\mathbf{k})}{\partial t} + \theta(\mathbf{k}) = - \int \frac{d^3 \mathbf{k}_1 d^3 \mathbf{k}_2}{(2\pi)^3} \delta_D(\mathbf{k} - \mathbf{k}_{12}) \alpha(\mathbf{k}_1, \mathbf{k}_2) \theta(\mathbf{k}_1) \delta(\mathbf{k}_2),$$

Velocity divergence

$$\theta = \nabla \cdot \mathbf{v} / (aH)$$

$$H^{-1} \frac{\partial \theta(\mathbf{k})}{\partial t} + \left\{ 2 + \frac{\dot{H}}{H^2} \right\} \theta(\mathbf{k}) + \frac{\kappa^2 \rho_m}{2H^2} \delta(\mathbf{k}) = - \frac{1}{2} \int \frac{d^3 \mathbf{k}_1 d^3 \mathbf{k}_2}{(2\pi)^3} \delta_D(\mathbf{k} - \mathbf{k}_{12}) \beta(\mathbf{k}_1, \mathbf{k}_2) \theta(\mathbf{k}_1) \theta(\mathbf{k}_2),$$

$$\alpha(\mathbf{k}_1, \mathbf{k}_2) = 1 + \frac{\mathbf{k}_1 \cdot \mathbf{k}_2}{|\mathbf{k}_1|^2}, \quad \beta(\mathbf{k}_1, \mathbf{k}_2) = \frac{(\mathbf{k}_1 \cdot \mathbf{k}_2) |\mathbf{k}_1 + \mathbf{k}_2|^2}{|\mathbf{k}_1|^2 |\mathbf{k}_2|^2}$$

Standard PT expansion ($|\delta|, |\theta| \ll 1$)

$$\delta(\mathbf{k}; t) = \delta^{(1)}(\mathbf{k}; t) + \delta^{(2)}(\mathbf{k}; t) + \dots, \quad \theta(\mathbf{k}; t) = \theta^{(1)}(\mathbf{k}; t) + \theta^{(2)}(\mathbf{k}; t) + \dots,$$

Standard PT kernel

Linear density field
(random Gaussian)

$$\delta^{(n)}(\mathbf{k}; t) = \int \frac{d^3 \mathbf{k}_1 \cdots d^3 \mathbf{k}_n}{(2\pi)^{3(n-1)}} \delta_D(\mathbf{k} - \mathbf{k}_{12\dots n}) \underline{F_n(\mathbf{k}_1, \dots, \mathbf{k}_n; t)} \delta_0(\mathbf{k}_1) \cdots \delta_0(\mathbf{k}_n),$$

$$\theta^{(n)}(\mathbf{k}; t) = \int \frac{d^3 \mathbf{k}_1 \cdots d^3 \mathbf{k}_n}{(2\pi)^{3(n-1)}} \delta_D(\mathbf{k} - \mathbf{k}_{12\dots n}) \underline{G_n(\mathbf{k}_1, \dots, \mathbf{k}_n; t)} \delta_0(\mathbf{k}_1) \cdots \delta_0(\mathbf{k}_n),$$

Power spectrum

Expression at next-to-leading order,

$$P^{(mn)} \simeq \langle \delta^{(m)} \delta^{(n)} \rangle$$

$$P_{\delta\delta}(k) = P^{(11)}(k) + \underline{\underline{P^{(22)}(k)}} + P^{(13)}(k)$$

Linear

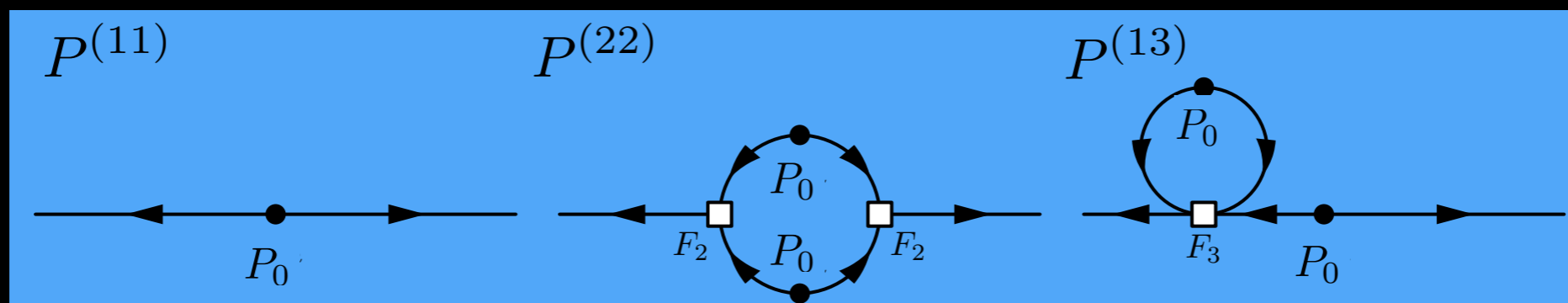
Next-to-leading order (1-loop)

$P^{(11)}(k) = P_0(k)$ Linearly extrapolated power spectrum

$$P^{(22)}(k) = 2 \int \frac{d^3\mathbf{q}}{(2\pi)^3} \{F_2(\mathbf{q}, \mathbf{k} - \mathbf{q})\}^2 P_0(q) P_0(|\mathbf{k} - \mathbf{q}|).$$

$$P^{(13)}(k) = 6 P_0(k) \int \frac{d^3\mathbf{q}}{(2\pi)^3} F_3(\mathbf{q}, -\mathbf{q}, \mathbf{k}) P_0(q)$$

Diagram representation



Next-to-next-to leading order

Expression at 2-loop order,

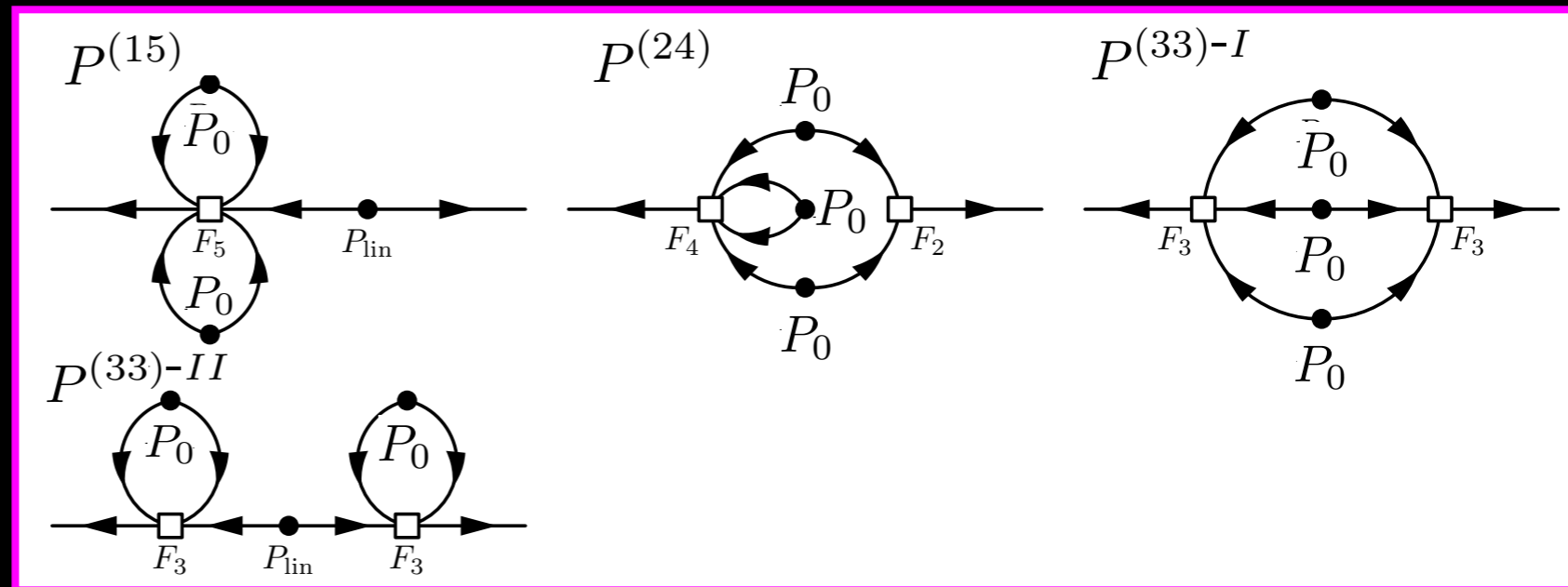
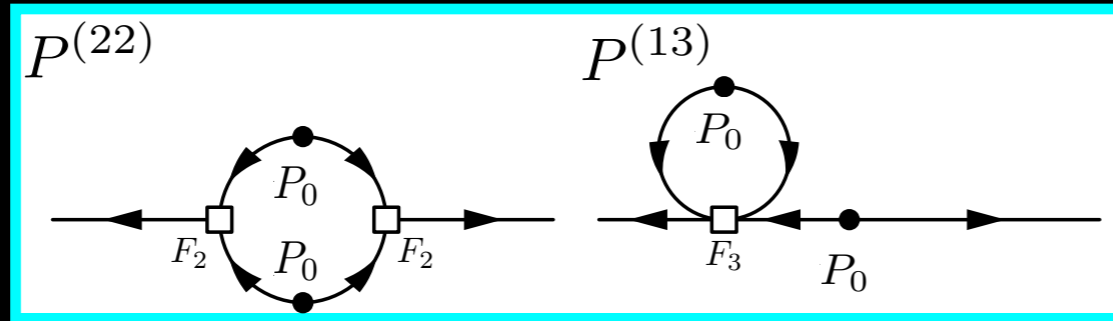
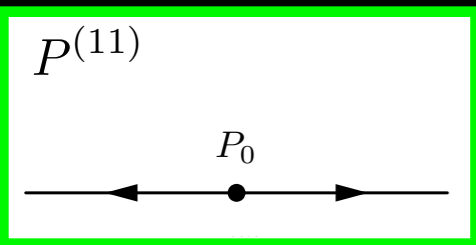
$$P^{(mn)} \simeq \langle \delta^{(m)} \delta^{(n)} \rangle$$

$$P(k) = \underbrace{P^{(11)}(k)}_{\text{Linear (tree)}} + \underbrace{\left(P^{(22)}(k) + P^{(13)}(k) \right)}_{\text{1-loop}} + \underbrace{\left(P^{(33)}(k) + P^{(24)}(k) + P^{(15)}(k) \right)}_{\text{2-loop}} + \dots$$

Linear (tree)

1-loop

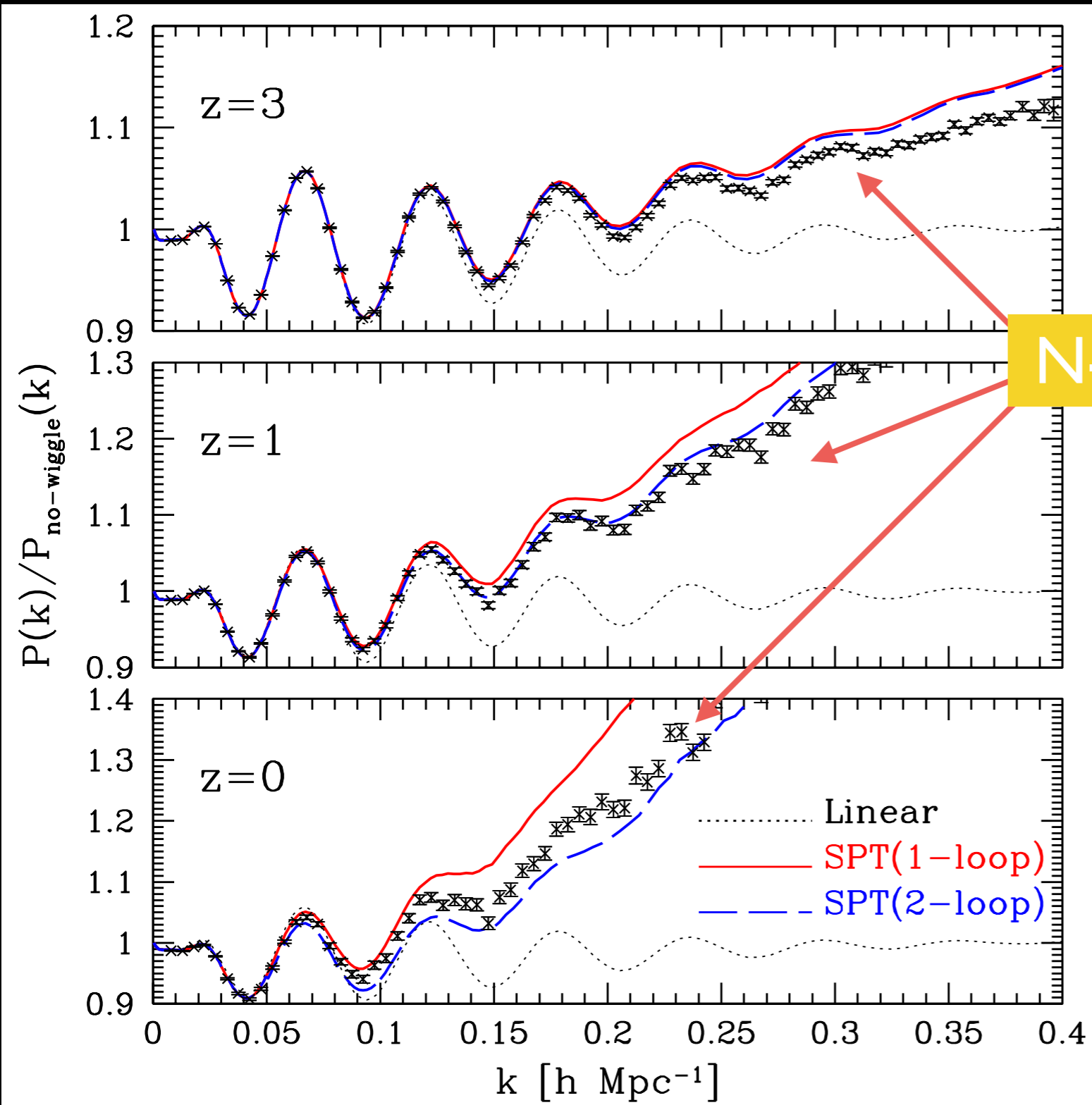
2-loop



Calculations involve multi-dimensional numerical integration,
but public code is now available (\rightarrow RegPT)

Standard PT power spectrum

AT et al. ('09)



N-body simulation

The results imply that standard PT produces ill-behaved PT expansion

→ need to be improved

Improving PT prediction

To cure a poor convergence of standard PT

→ Reorganize standard PT expansion



Concept of '*propagator*' in physics/mathematics is useful :

$$\delta_0(k)$$

initial density field (Gaussian)

power spectrum

$$P_0(k)$$

from linear theory
(CMB Boltzmann code)

$$\delta(k; z)$$

Evolved density field (non-Gaussian)

Observables

$$P(k; z)$$

$$B(k_1, k_2, k_3; z)$$

⋮

of dark matter/galaxies/halos

propagator

Improving PT prediction

To cure a poor convergence of standard PT

→ Reorganize standard PT expansion



Concept of '*propagator*' in physics/mathematics is useful :

Propagator carries statistical info. on nonlinear mode-coupling

Evolved (non-linear) density field

Crocce & Scoccimarro ('06)

$$\left\langle \frac{\delta \delta_m(\mathbf{k}; t)}{\delta \delta_0(\mathbf{k}')} \right\rangle \equiv \delta_D(\mathbf{k} - \mathbf{k}') \Gamma^{(1)}(\mathbf{k}; t) \quad \text{Propagator}$$

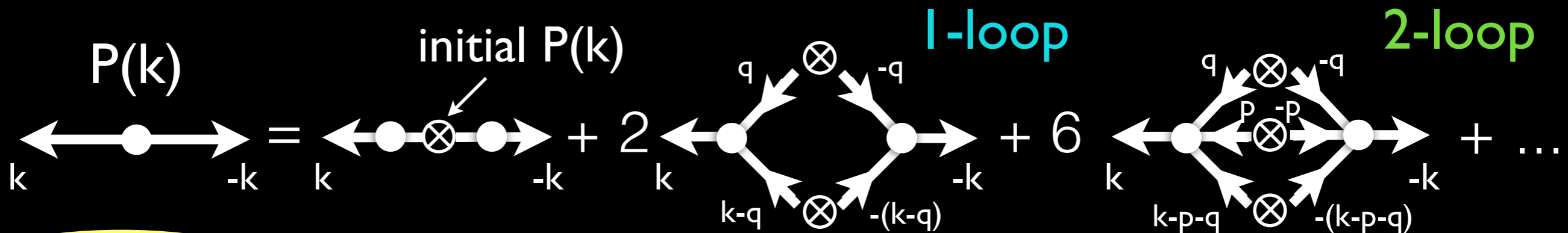
Initial density field

Ensemble w.r.t randomness of initial condition

Power spectrum

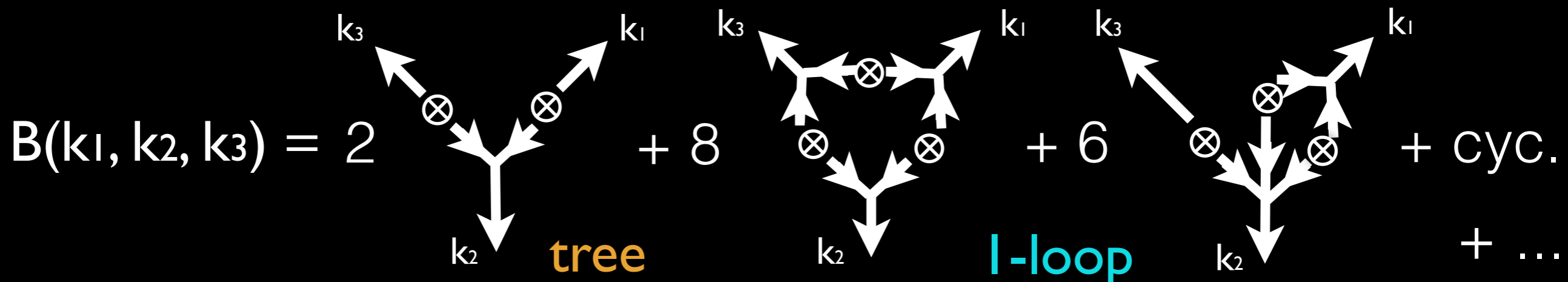
initial power spectrum

$$P(k; t) = \left[\Gamma^{(1)}(k; t) \right]^2 P_0(k) + 2 \int \frac{d^3 \mathbf{q}}{(2\pi)^3} \left[\Gamma^{(2)}(\mathbf{q}, \mathbf{k} - \mathbf{q}; t) \right]^2 P_0(q) P_0(|\mathbf{k} - \mathbf{q}|) + 6 \int \frac{d^6 \mathbf{p} d^3 \mathbf{q}}{(2\pi)^6} \left[\Gamma^{(3)}(\mathbf{p}, \mathbf{q}, \mathbf{k} - \mathbf{p} - \mathbf{q}; t) \right]^2 P_0(p) P_0(q) P_0(|\mathbf{k} - \mathbf{p} - \mathbf{q}|) + \dots$$



Bispectrum

$$B(k_1, k_2, k_3) = 2 \Gamma^{(2)}(\mathbf{k}_1, \mathbf{k}_2) \Gamma^{(1)}(k_1) \Gamma^{(1)}(k_2) P_0(k_1) P_0(k_2) + \text{cyc.} + \left[8 \int d^3 q \Gamma^{(2)}(\mathbf{k}_1 - \mathbf{q}, \mathbf{q}) \Gamma^{(2)}(\mathbf{k}_2 + \mathbf{q}, -\mathbf{q}) \Gamma^{(2)}(\mathbf{q} - \mathbf{k}_1, -\mathbf{k}_2 - \mathbf{q}) P_0(|\mathbf{k}_1 - \mathbf{q}|) P_0(|\mathbf{k}_2 + \mathbf{q}|) P_0(q) + 6 \int d^3 q \Gamma^{(3)}(-\mathbf{k}_3, -\mathbf{k}_2 + \mathbf{q}, -\mathbf{q}) \Gamma^{(2)}(\mathbf{k}_2 - \mathbf{q}, \mathbf{q}) \Gamma^{(1)}(\mathbf{k}_3) P_0(|\mathbf{k}_2 - \mathbf{q}|) P_0(q) P_0(k_3) + \text{cyc.} \right].$$

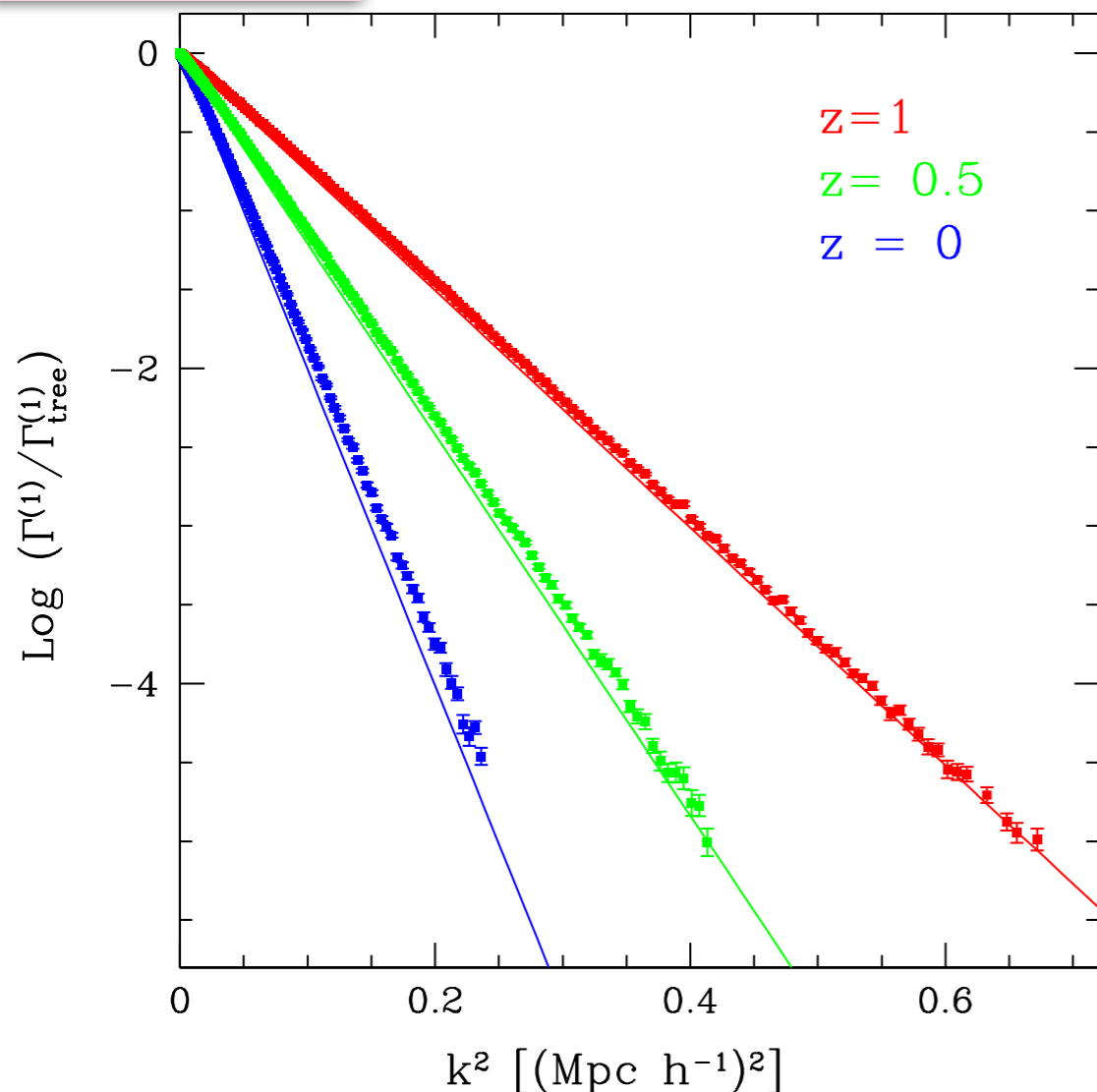


Generic properties

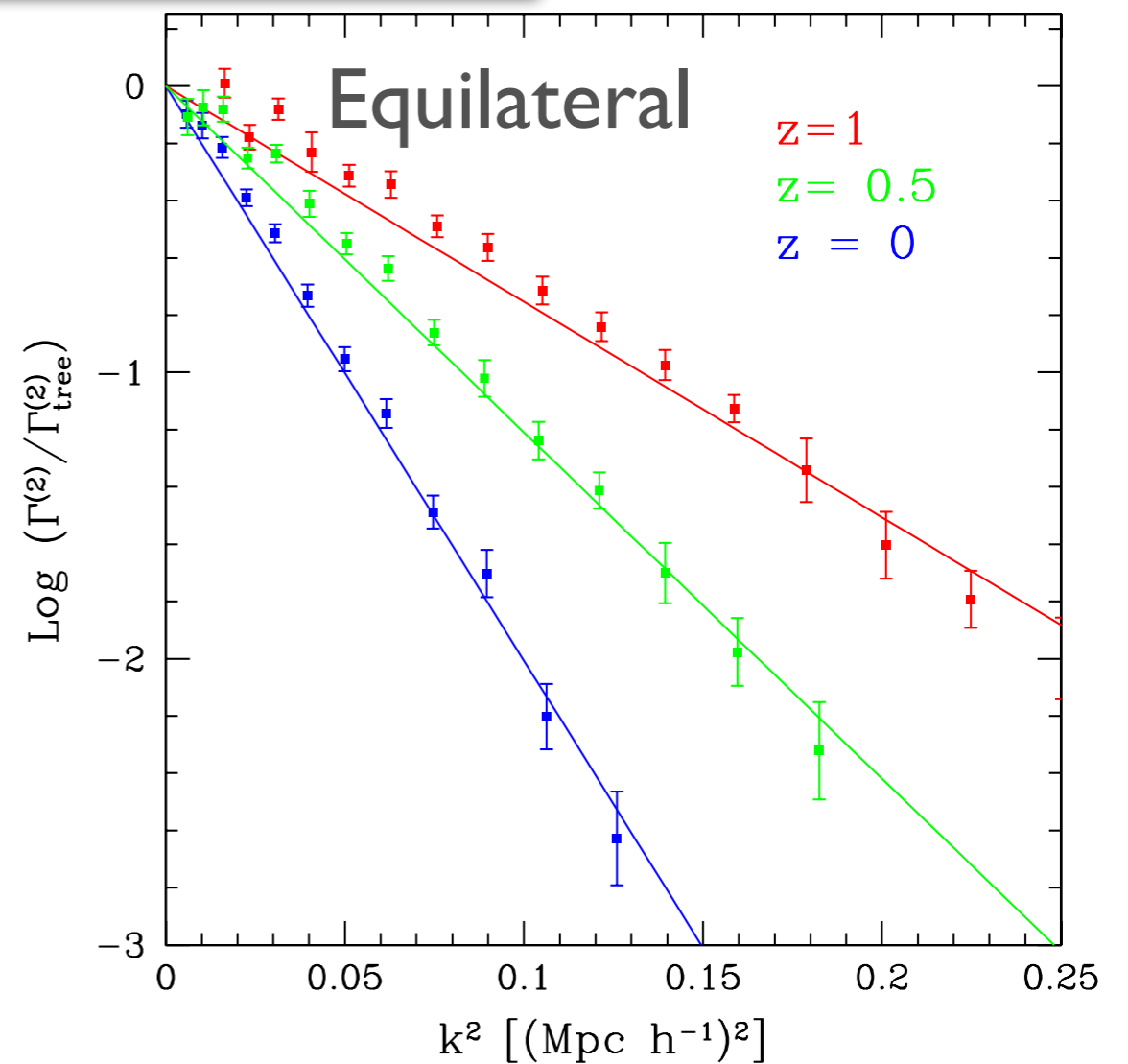
Crocce & Scoccimarro '06, Bernardeau et al. '08

$$\Gamma^{(n)} \xrightarrow{k \rightarrow +\infty} \Gamma_{\text{tree}}^{(n)} e^{-k^2 \sigma_v^2 / 2} \quad ; \quad \sigma_v^2 = \int \frac{dq}{6\pi^2} P_{\theta\theta}(q)$$

$\Gamma^{(1)}(k)$



$\Gamma^{(2)}(k_1, k_2, k_3)$

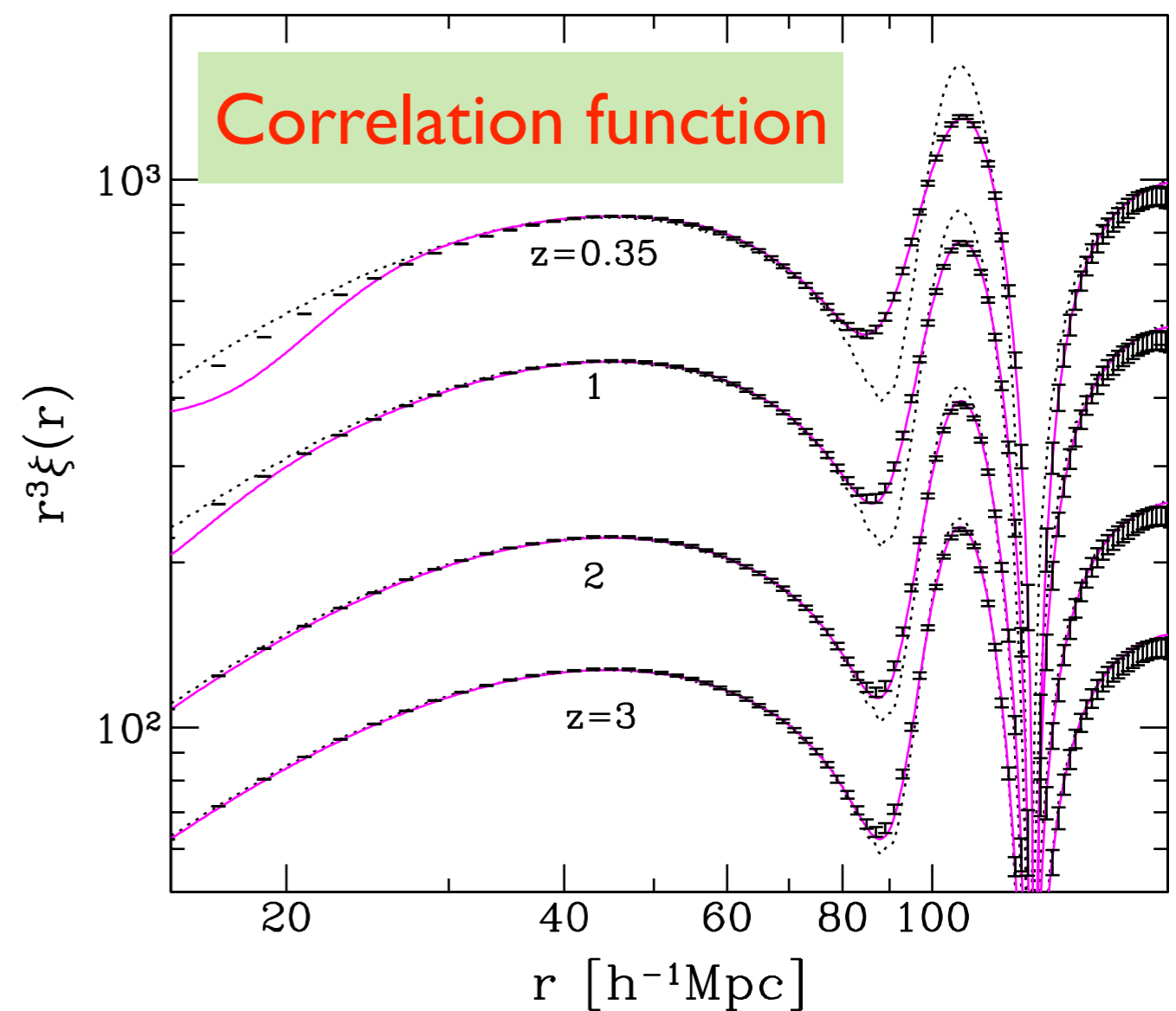
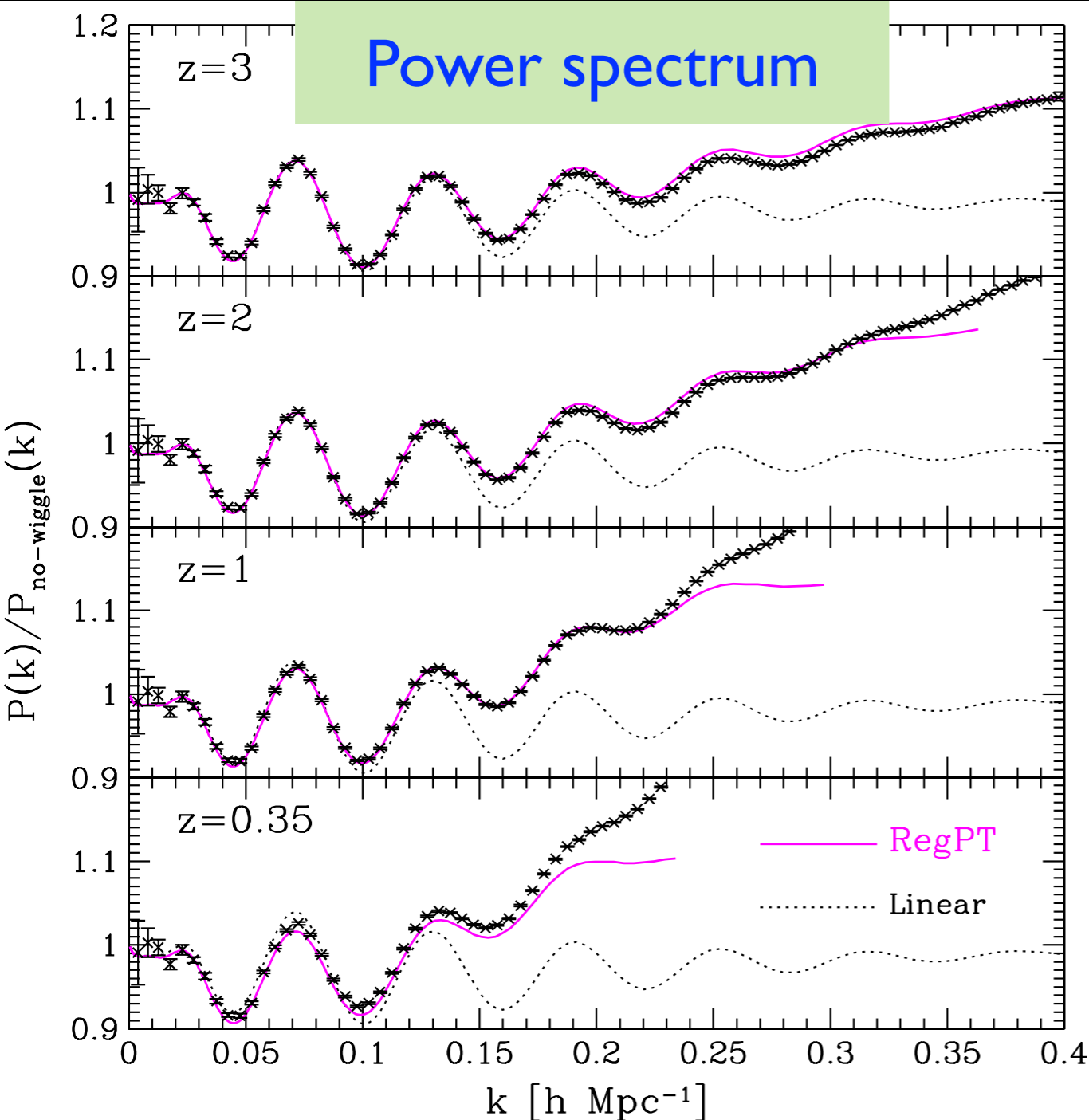


RegPT : fast PT code for $P(k)$ & $\xi(r)$

few sec.

A **public code** based on multi-point propagators at **2-loop order**

http://www2.yukawa.kyoto-u.ac.jp/~atsushi.taruya/regpt_code.html



AT, Bernardeau, Nishimichi & Codis ('12)

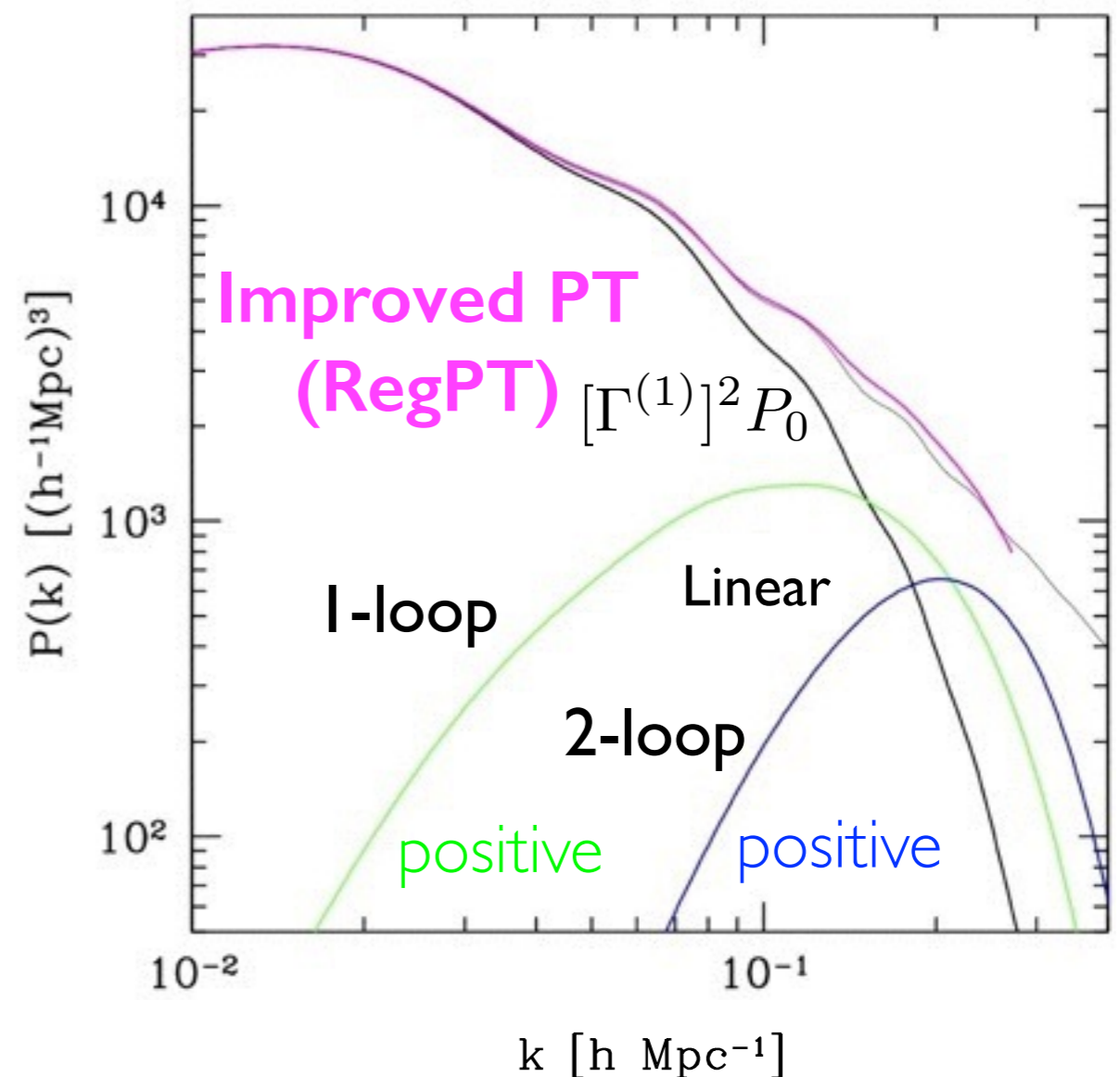
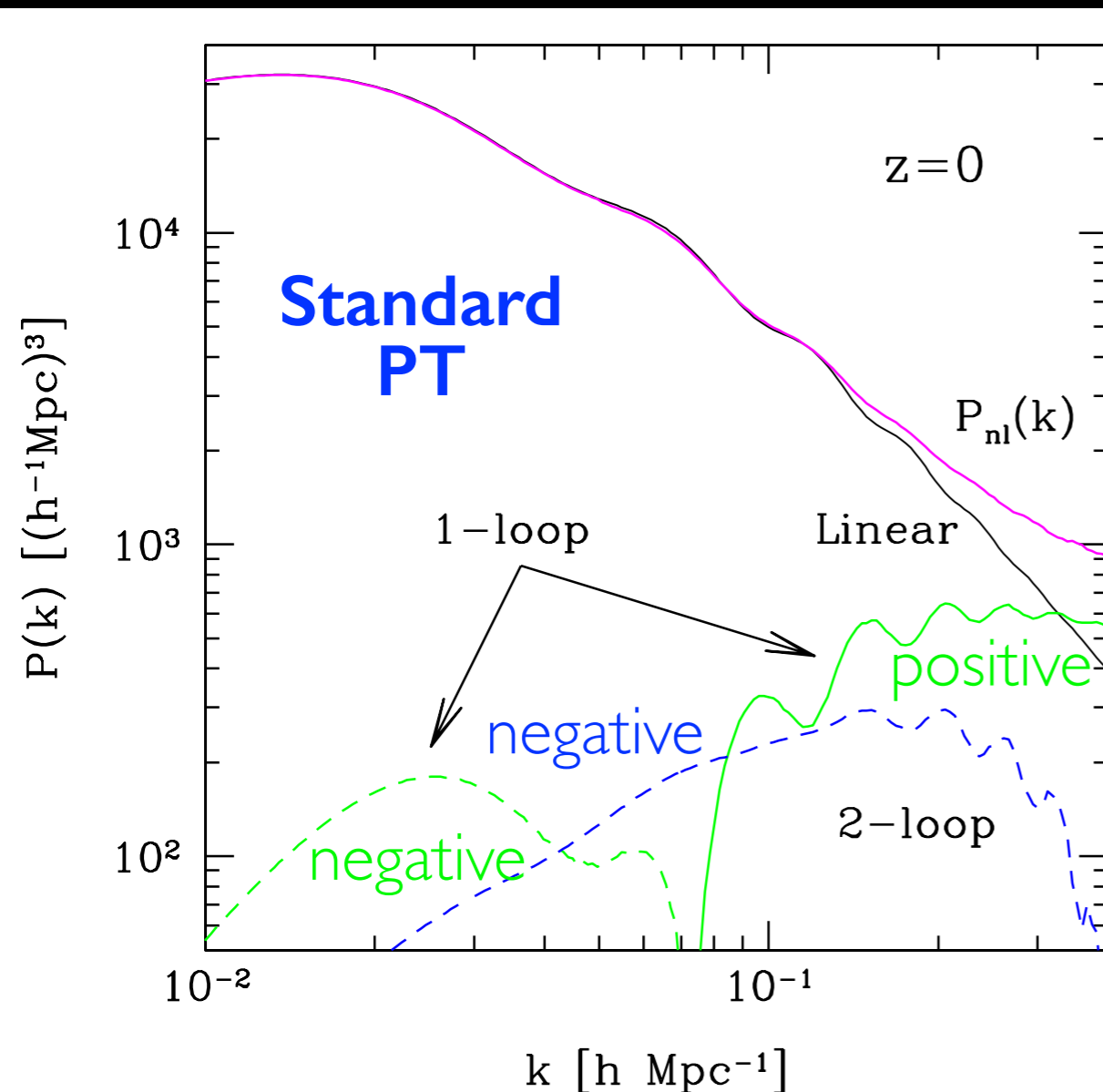
Why improved PT works well ?

AT, Bernardeau, Nishimichi, Codis ('12)

AT et al. ('09)

- All corrections become comparable at low- z .
- Positivity is not guaranteed.

Corrections are positive & localized, shifted to higher- k for higher-loop

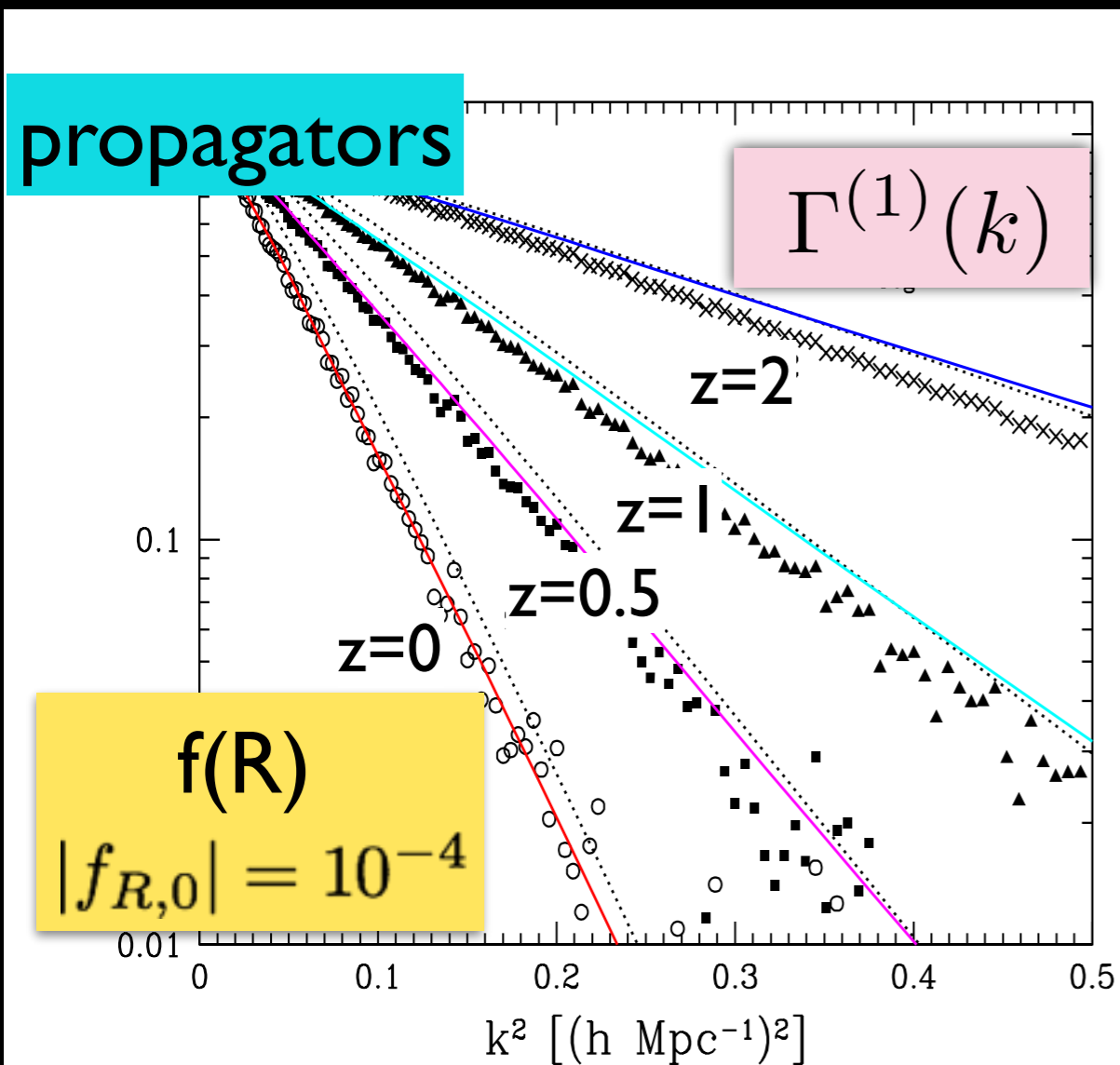


RegPT in modified gravity

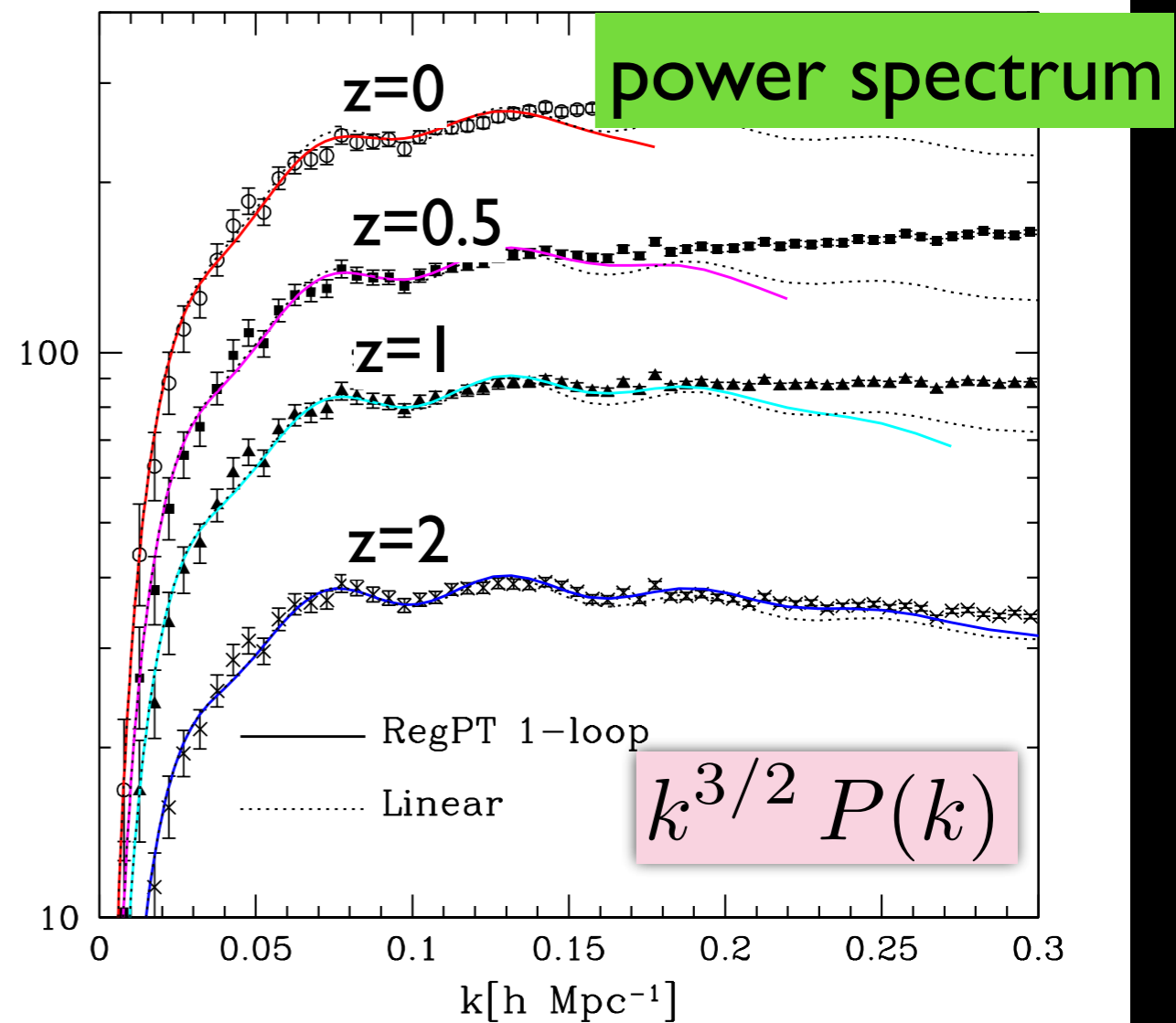
Good convergence is ensured by

a *generic* damping behavior in propagators $\Gamma^{(n)} \xrightarrow{k \rightarrow \infty} \Gamma_{\text{tree}}^{(n)} e^{-k^2 \sigma_d^2/2}$

Even in modified gravity, well-controlled expansion with RegPT



N-body data: Baojiu Li

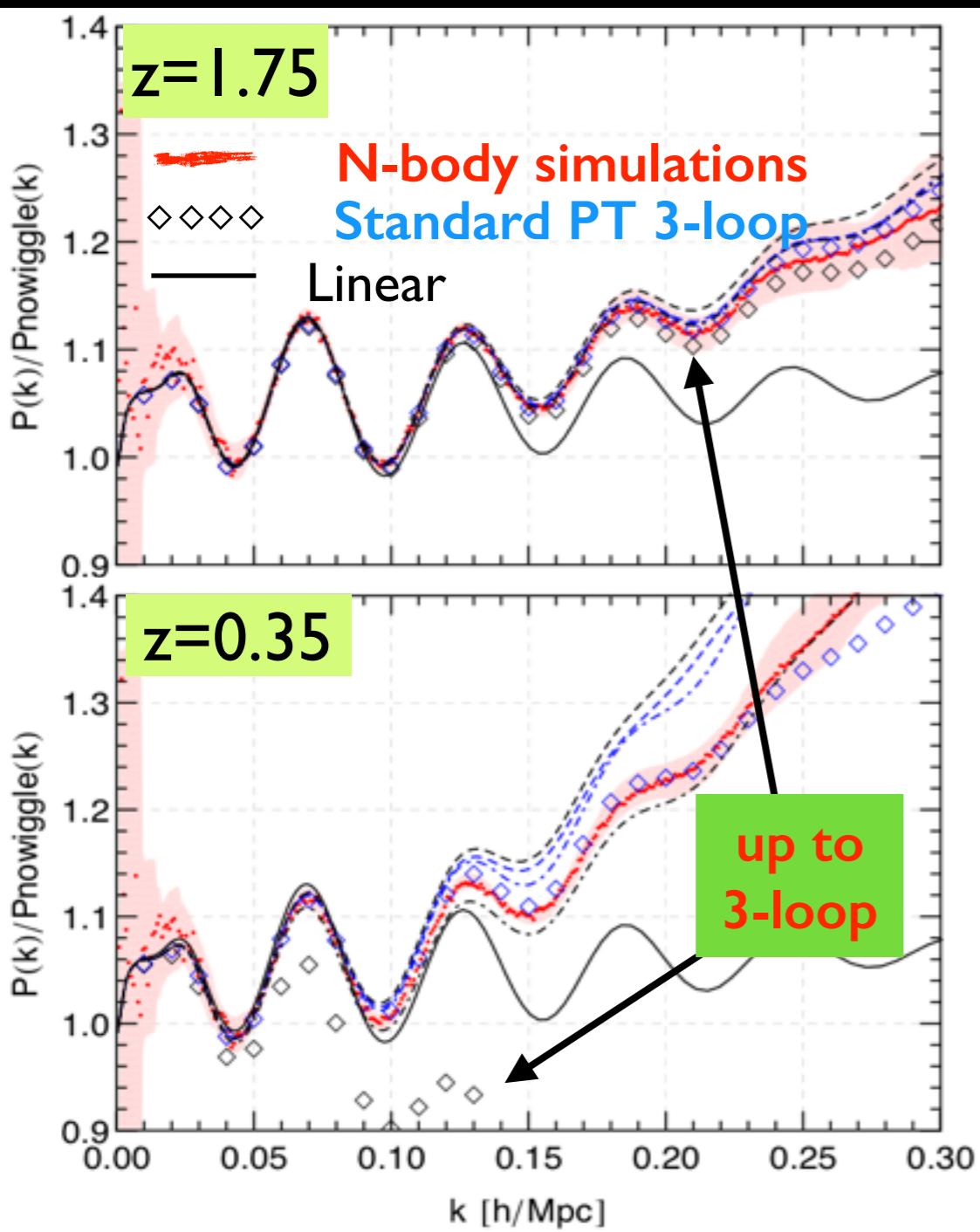


AT, Nishimichi, Bernardeau, et al. ('14)



Curse of UV divergence

Further including higher-order (i.e., 3-loop), can we use PT template more aggressively? \longrightarrow wide fitting range for a large k_{\max}



A very big correction at low-k

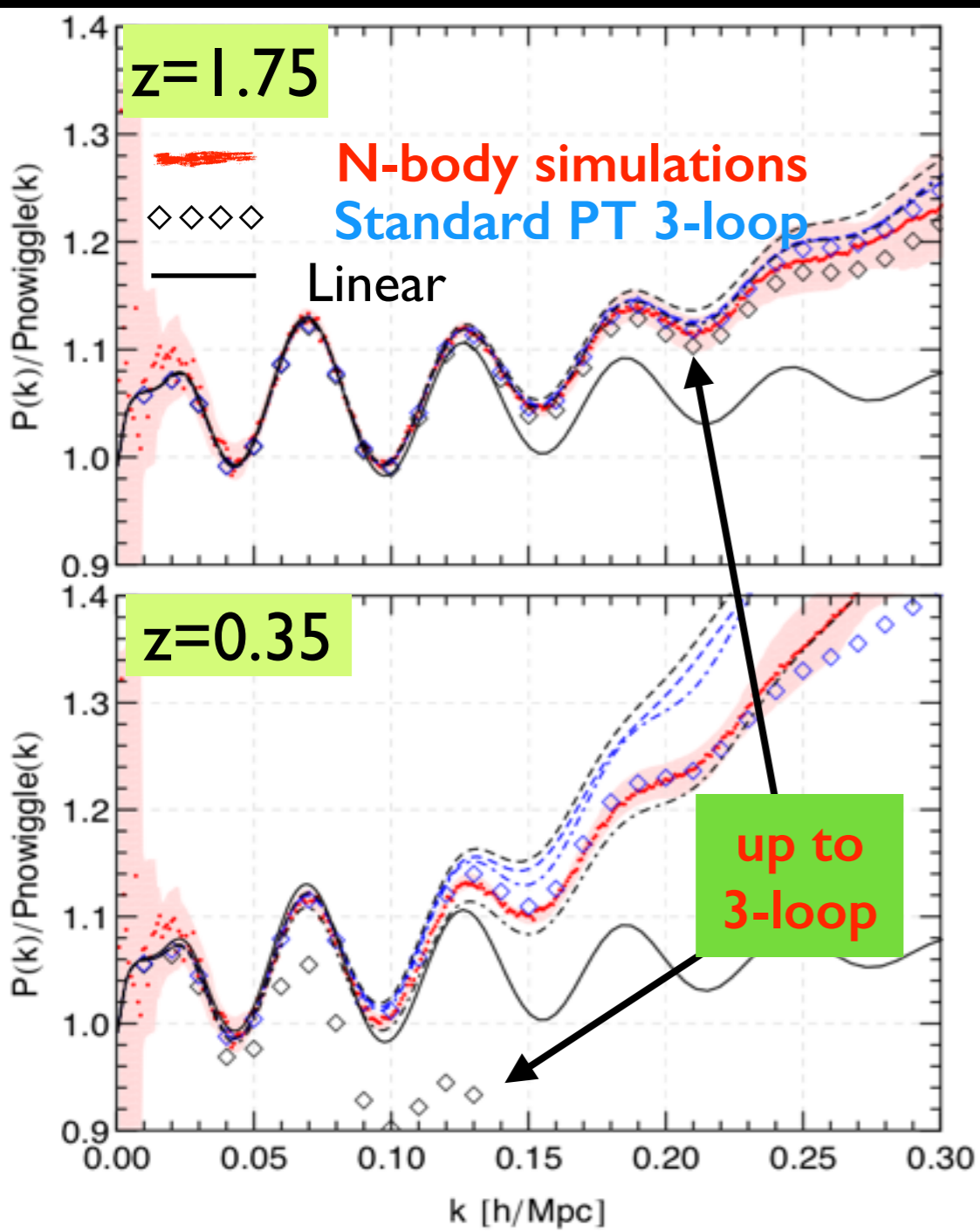
----- Break down of PT ?

This is not only the case of SPT
but also most of resummed PTs



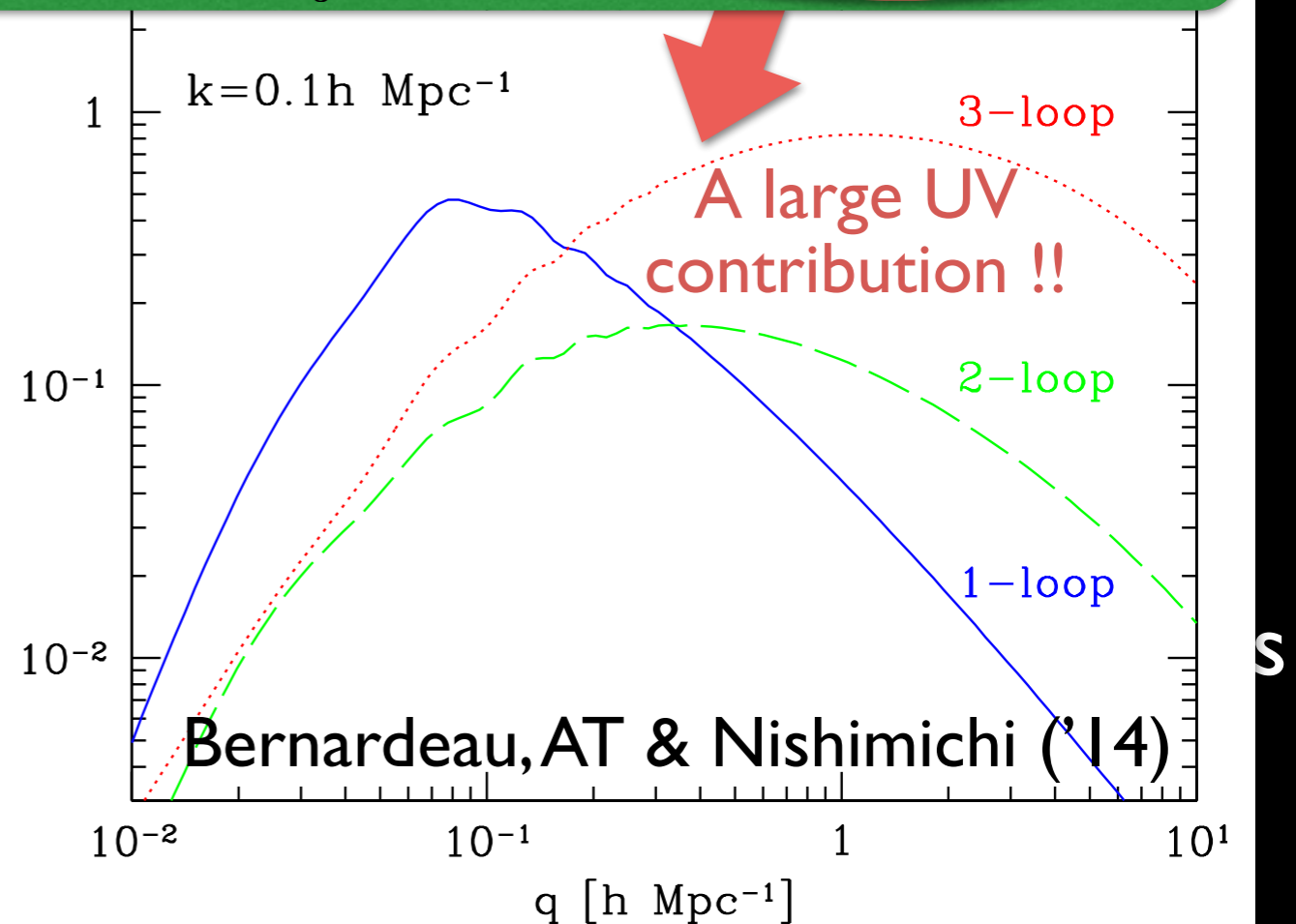
Curse of UV divergence

Further including higher-order (i.e., 3-loop), can we use PT template more aggressively? \longrightarrow wide fitting range for a large k_{\max}



Each higher-order term involves mode-coupling integral:

$$P_{n\text{-loop}}(k) \propto \int d \ln q K_{n\text{-loop}}(k, q) P_0(q)$$



Nature of nonlinear response

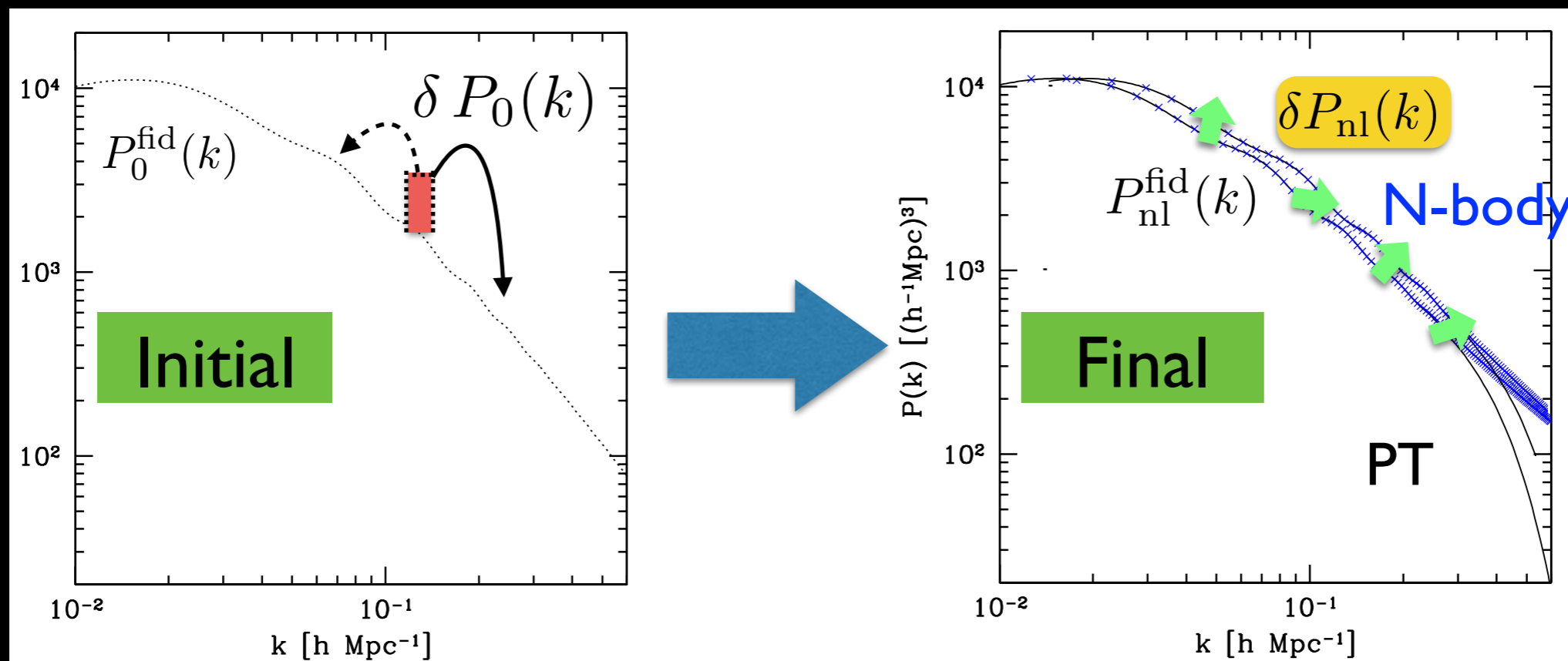
Nishimichi, Bernardeau & AT (arXiv:1411.2970)

Q How does the mode-coupling structure look like in reality ?

Nonlinear response
we will measure

$$\delta P_{\text{nl}}(k) = \int d \ln q K(k, q) \delta P_0(q)$$

➔ How the small disturbance added in initial power spectrum can contribute to each Fourier mode in final power spectrum



Nature of nonlinear response

Nishimichi, Bernardeau & AT (arXiv:1411.2970)

Q How does the mode-coupling structure look like in reality ?

Nonlinear response
we will measure

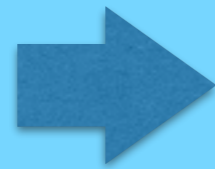
$$\delta P_{\text{nl}}(k) = \int d \ln q K(k, q) \delta P_0(q)$$

How the small disturbance added in initial power spectrum can contribute to each Fourier mode in final power spectrum

Alternative definition

(discretized) estimator

$$K(k, q) = q \frac{\delta P_{\text{nl}}(k)}{\delta P_0(q)}$$



$$\hat{K}(k_i, q_j) P_0(q_j) \equiv \frac{P_{\text{nl}}^+(k_i) - P_{\text{nl}}^-(k_i)}{\Delta \ln P_0 \Delta \ln q}$$

name	box	particles	z_{start}	soft	mass	bins	runs	total
L9-N10	512	1024^3	63	25	0.97	5	1	10
L9-N9	512	512^3	31	50	7.74	15	4	120
L9-N8	512	256^3	15	100	61.95	13	4	104
L10-N9	1024	512^3	31	100	61.95	15	1	30

$$\Delta \ln q = \ln q_{j+1} - \ln q_j$$

Run many simulations...

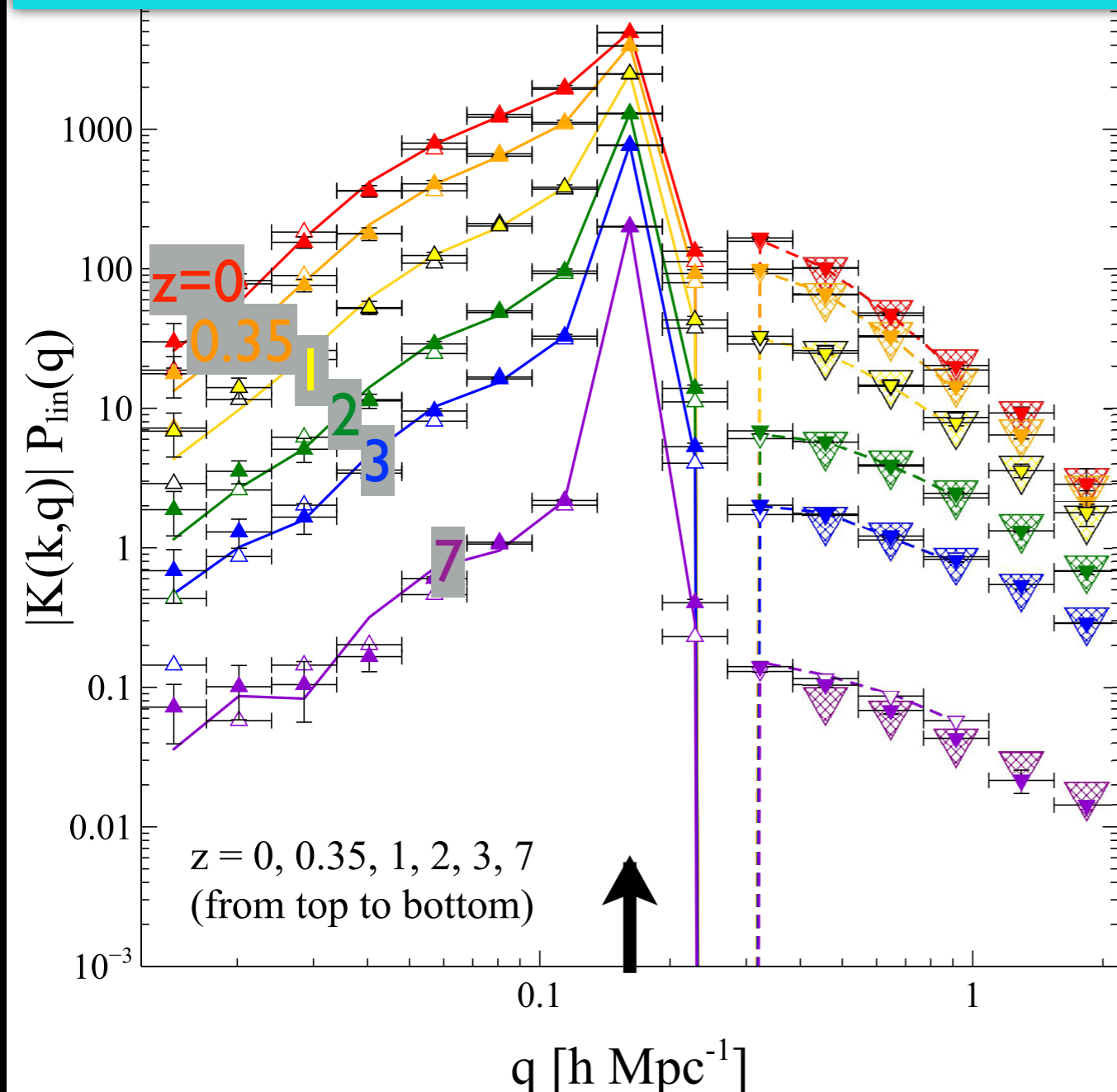
by T.Nishimishi

Measurement result

Nishimichi, Bernardeau & AT (arXiv:1411.2970)

Nonlinear response to a small initial variation in $P(k)$:

$$\delta P_{\text{nl}}(k) = \int d \ln q K(k, q) \delta P_0(q)$$



Measured at
 $k=0.162 \text{ [h/Mpc]}$

▲ or — : positive
▼ or - - - : negative

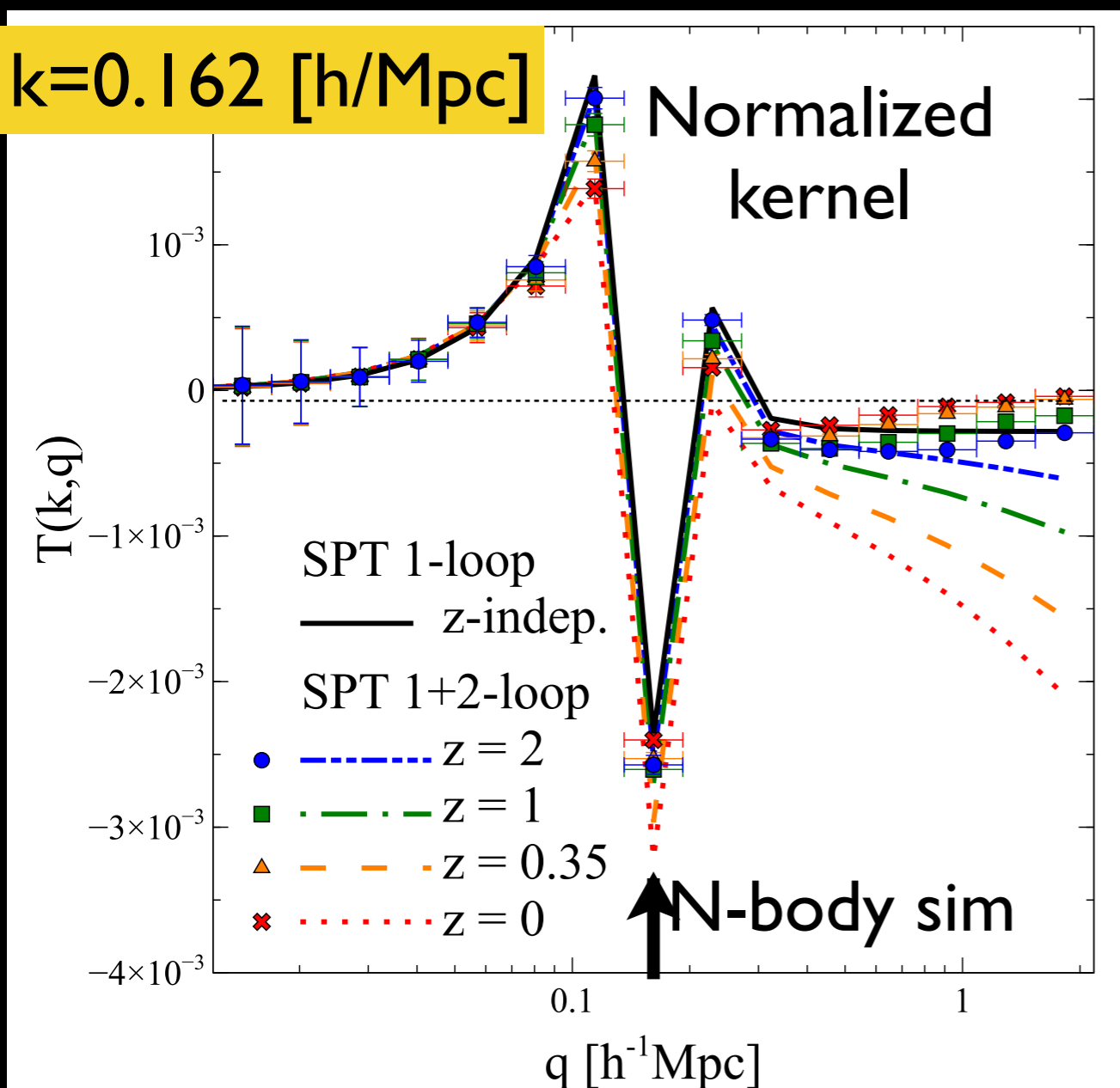
FIG. 1: Response function measured from simulations. We plot $|K(k, q)| P^{\text{lin}}(q)$ as a function of the linear mode q for a fixed nonlinear mode at $k = 0.161 h \text{ Mpc}^{-1}$ indicated by the vertical arrow. The filled (open) symbols show L9-N9 (L10-N9), the lines depict L9-N8, while the big hatched symbols on small scales are L9-N10. Positive (negative) values are indicated as the upward (downward) triangles or the solid (dashed) lines.

Response function in simulations

Nishimichi, Bernardeau & AT (arXiv:1411.2970)

$$T(k, q)$$

$$= [K(k, q) - K_{\text{lin}}(k, q)] / [q P_{\text{lin}}(k)]$$



Black solid : Standard PT 1-loop
(z-indep.)

Blue, Green, Orange, Red : 2-loop



$q < k$: reproduce simulation well

$q > k$: discrepancy is manifest
(particularly large at low-z)

UV contribution is suppressed
in N-body simulation!!

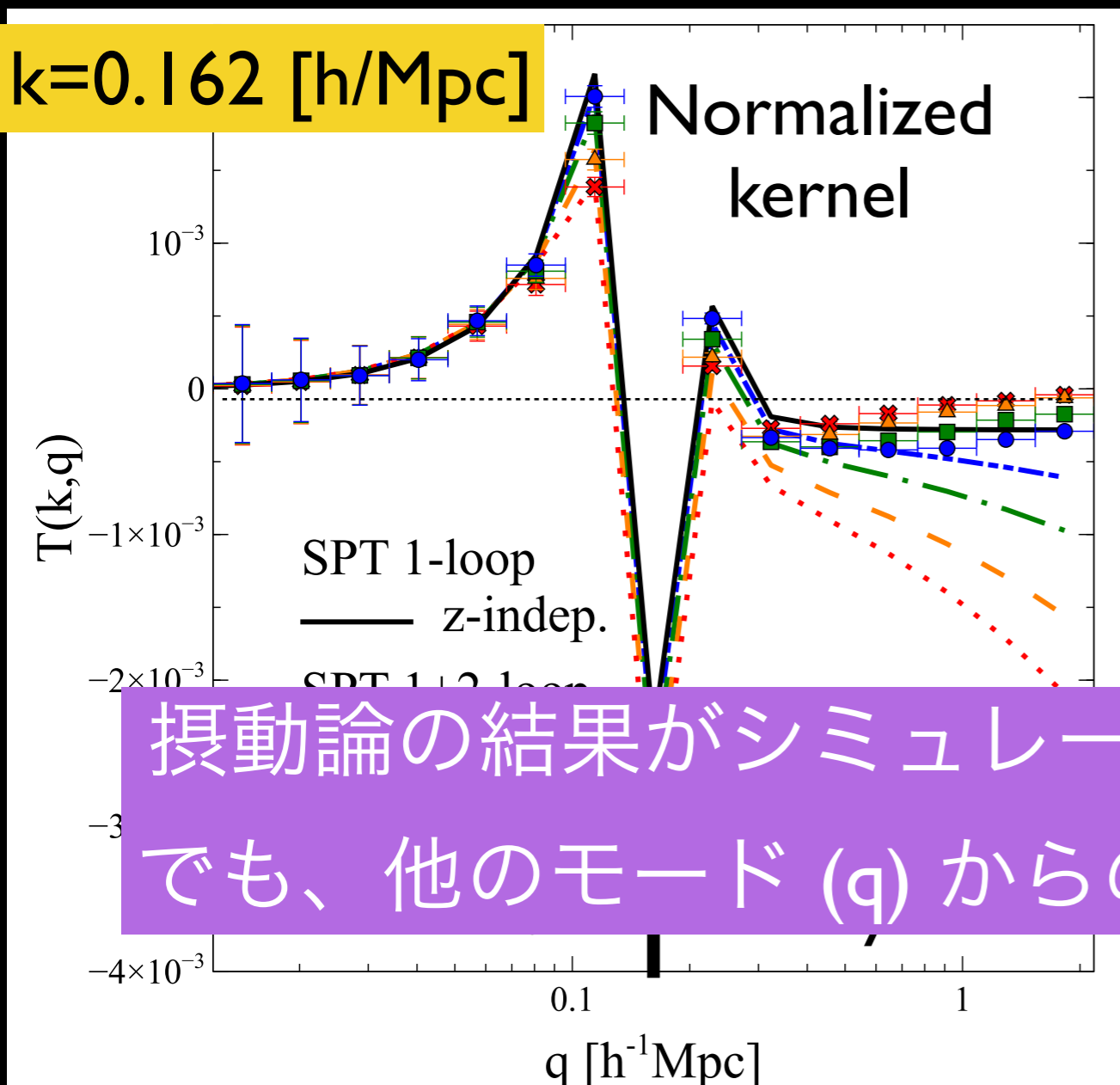
Response function in simulations

Nishimichi, Bernardeau & AT (arXiv:1411.2970)

$$T(k, q)$$

$$= [K(k, q) - K_{\text{lin}}(k, q)] / [q P_{\text{lin}}(k)]$$

$k=0.162$ [h/Mpc]



Black solid : Standard PT 1-loop
(z-indep.)

Blue, Green, Orange, Red : 2-loop



$q < k$: reproduce simulation well

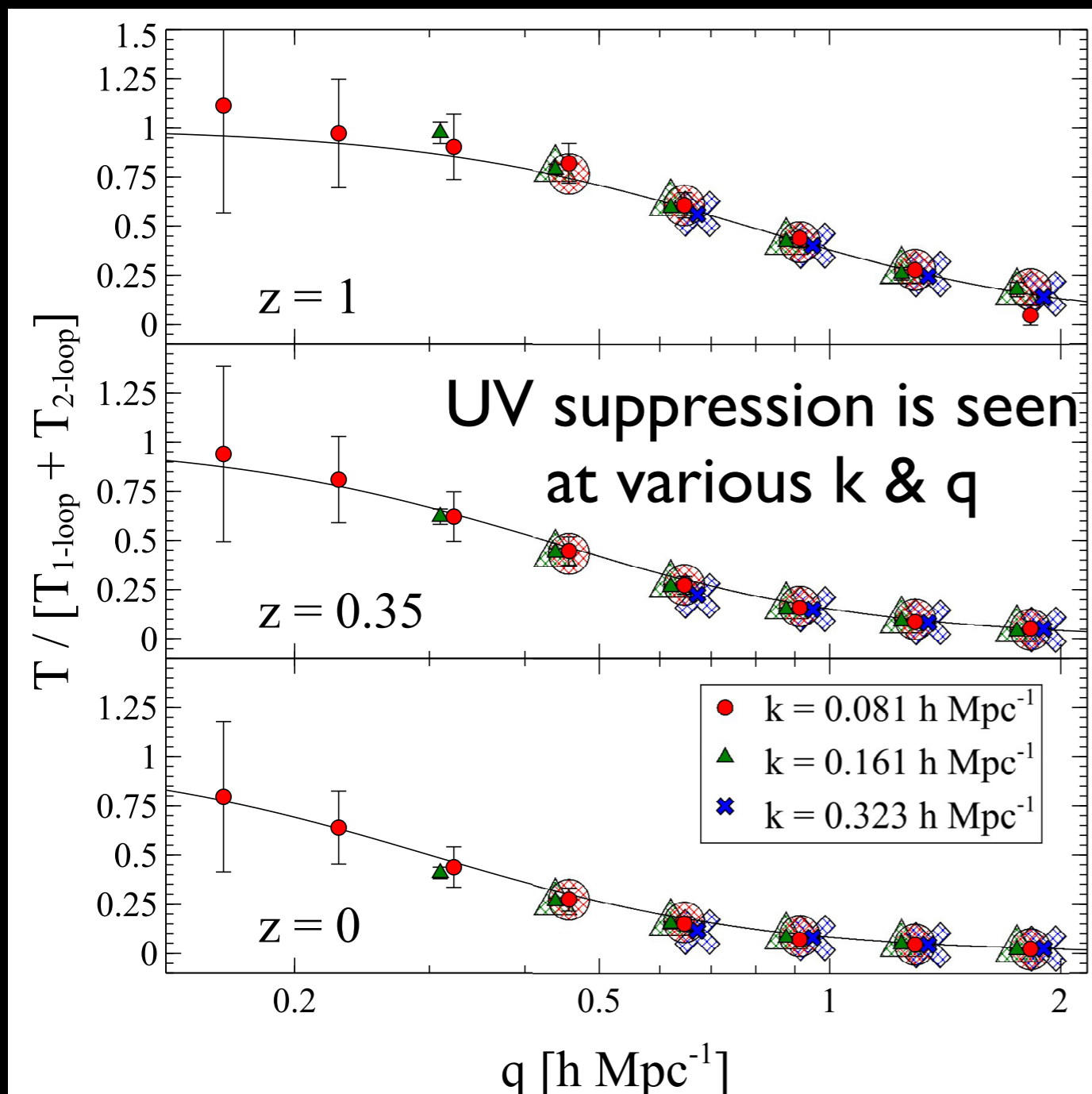
摂動論の結果がシミュレーションとよく合う波数領域 (k)
でも、他のモード (q) からの応答をみると「ずれ」がある

UV contribution is suppressed
in N-body simulation!!

Characterizing UV suppression

Nishimichi, Bernardeau & AT (arXiv:1411.2970)

$$T(k, q) = [K(k, q) - K^{\text{lin}}(k, q)] / [qP^{\text{lin}}(k)]$$



← ratio of measured response function to PT prediction

Fitting formula

$$K_{\text{eff}}(k, q) = [K^{1\text{-loop}}(k, q) + K^{1\text{-loop}}(k, q)] \frac{1}{1 + (q/q_0)^2}$$

$q_0(z) = 0.3/D_+^2(z) [h \text{ Mpc}^{-1}]$

$K^{1\text{-loop}}, K^{1\text{-loop}}$: Standard PT kernel

Some physical mechanism works, and controls the mode transfer

EFT cures PT predictions ?

UV suppression is definitely attributed to small-scale physics, which cannot be described by current PT treatment

(formation & merging processes of dark matter halos, ...)

Effective field theory (EFT) of large-scale structure

Phenomenologically introduce viscosity & anisotropic stress to characterize deviations from pressureless & irrotational fluid

$$\frac{\partial \delta}{\partial t} + \frac{1}{a} \nabla \cdot [(1 + \delta) \mathbf{v}] = 0,$$

$$\frac{\partial \mathbf{v}}{\partial t} + H \mathbf{v} + \frac{1}{a} (\mathbf{v} \cdot \nabla) \cdot \mathbf{v} = -\frac{1}{a} \nabla \psi - \frac{1}{\rho_m} \frac{1}{a} \nabla \tau_{ij}$$

$$\frac{1}{a^2} \nabla^2 \psi = \frac{\kappa^2}{2} \rho_m \delta$$



Baumann et al. ('12), Carrasco, Herzberg & Senatore ('12), Carrasco et al. ('13ab), Porto, Senatore & Zaldarriaga ('14), ...

but need a calibration with N-body simulation

EFT cures PT predictions ?

UV suppression is definitely attributed to small-scale physics, which cannot be described by current PT treatment

Leading-order EFT corrections

e.g., Herzberg ('14)

$$\tau_{ij} = \rho_m \left[\left(c_s^2 \delta - \frac{c_{bv}^2}{aH} \nabla \cdot \mathbf{v} \right) \delta_{ij} - \frac{3}{4} \frac{c_{sv}^2}{aH} \left\{ \partial_j v_i + \partial_i v_j - \frac{2}{3} (\nabla \cdot \mathbf{v}) \delta_{ij} \right\} \right]$$

Does this really help PT prediction ?

$$\frac{\partial \delta}{\partial t} + \frac{1}{a} \nabla \cdot [(1 + \delta) \mathbf{v}] = 0,$$

$$\frac{\partial \mathbf{v}}{\partial t} + H \mathbf{v} + \frac{1}{a} (\mathbf{v} \cdot \nabla) \cdot \mathbf{v} = -\frac{1}{a} \nabla \psi - \frac{1}{\rho_m} \frac{1}{a} \nabla \tau_{ij}$$

$$\frac{1}{a^2} \nabla^2 \psi = \frac{\kappa^2}{2} \rho_m \delta$$

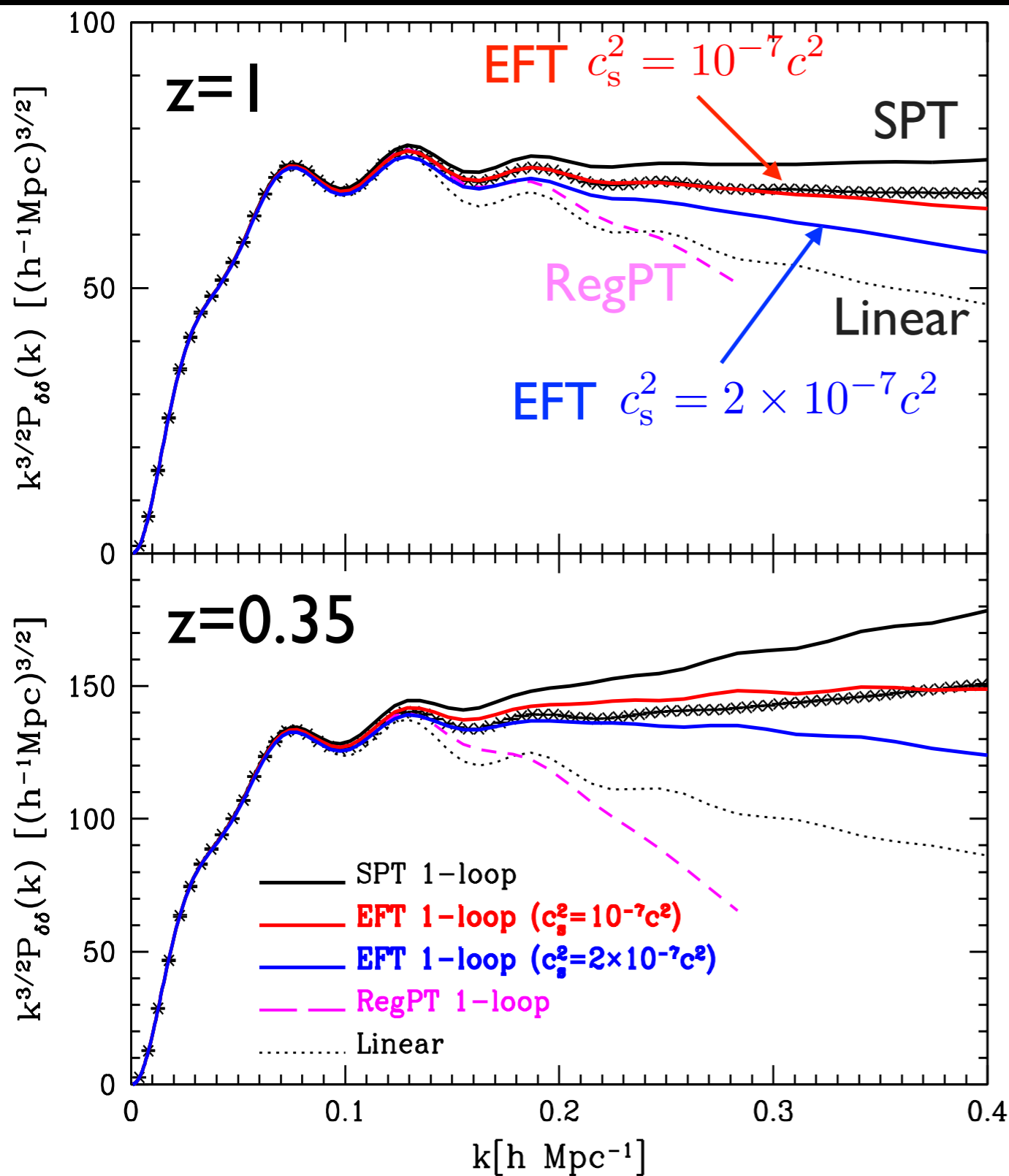


Baumann et al. ('12), Carrasco, Herzberg & Senatore ('12), Carrasco et al. ('13ab), Porto, Senatore & Zaldarriaga ('14),

but need a calibration with N-body simulation

...

Testing EFT approach (1-loop)



Assuming irrotationality,

shear & bulk viscosities

are degenerate: $c_v^2 \equiv c_{bv}^2 + c_{sv}^2$

At 1-loop order,

corrections are approximately described by a single-parameter:

$$c_s^2 + f c_v^2$$

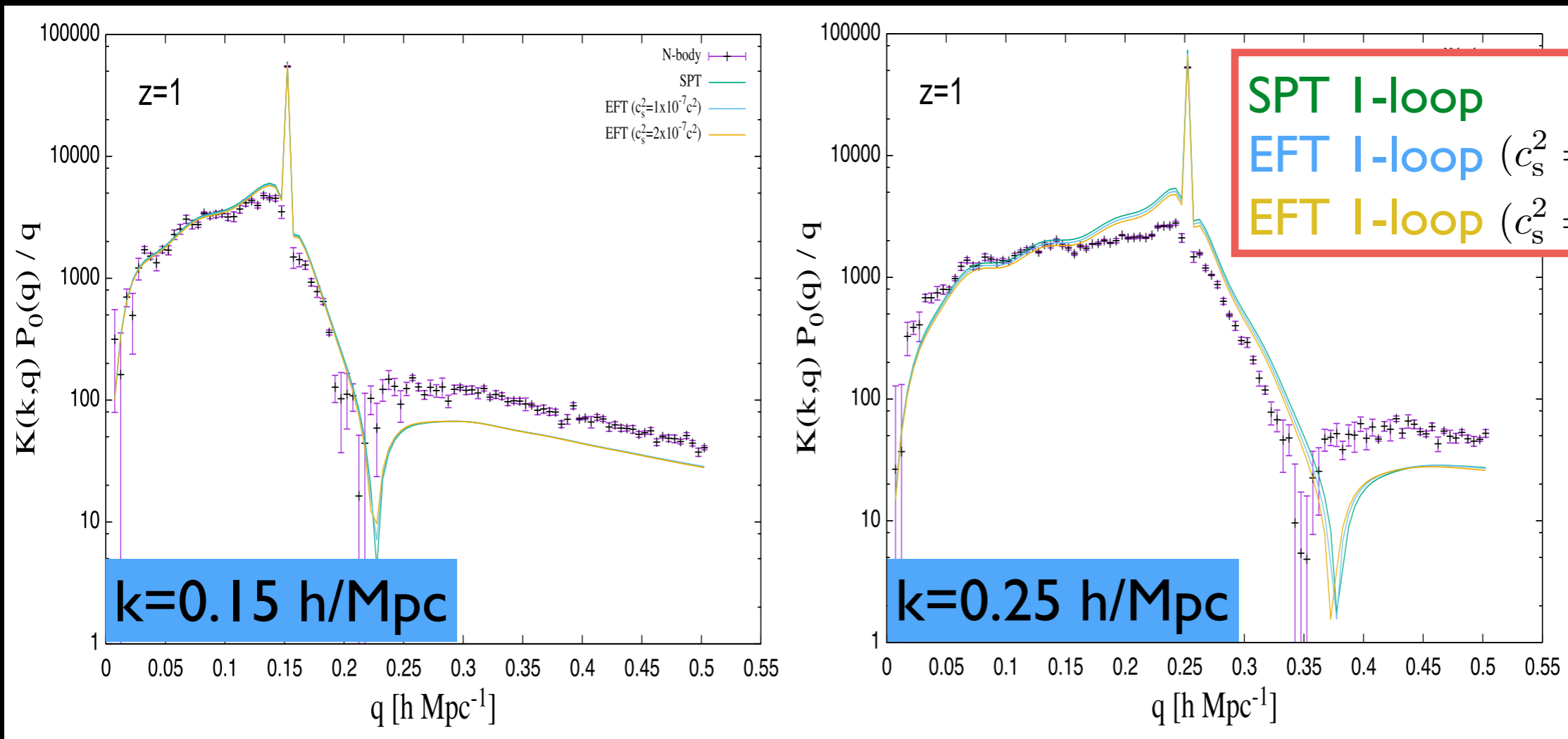
Allowing the parameter c_s to be free, PT predictions *superficially* reproduce N-body results well

BUT !!

Testing EFT approach (1-loop)

Response function
of $P(k)$

$$K(k, q) = q \frac{\delta P_{\text{nl}}(k)}{\delta P_0(q)}$$

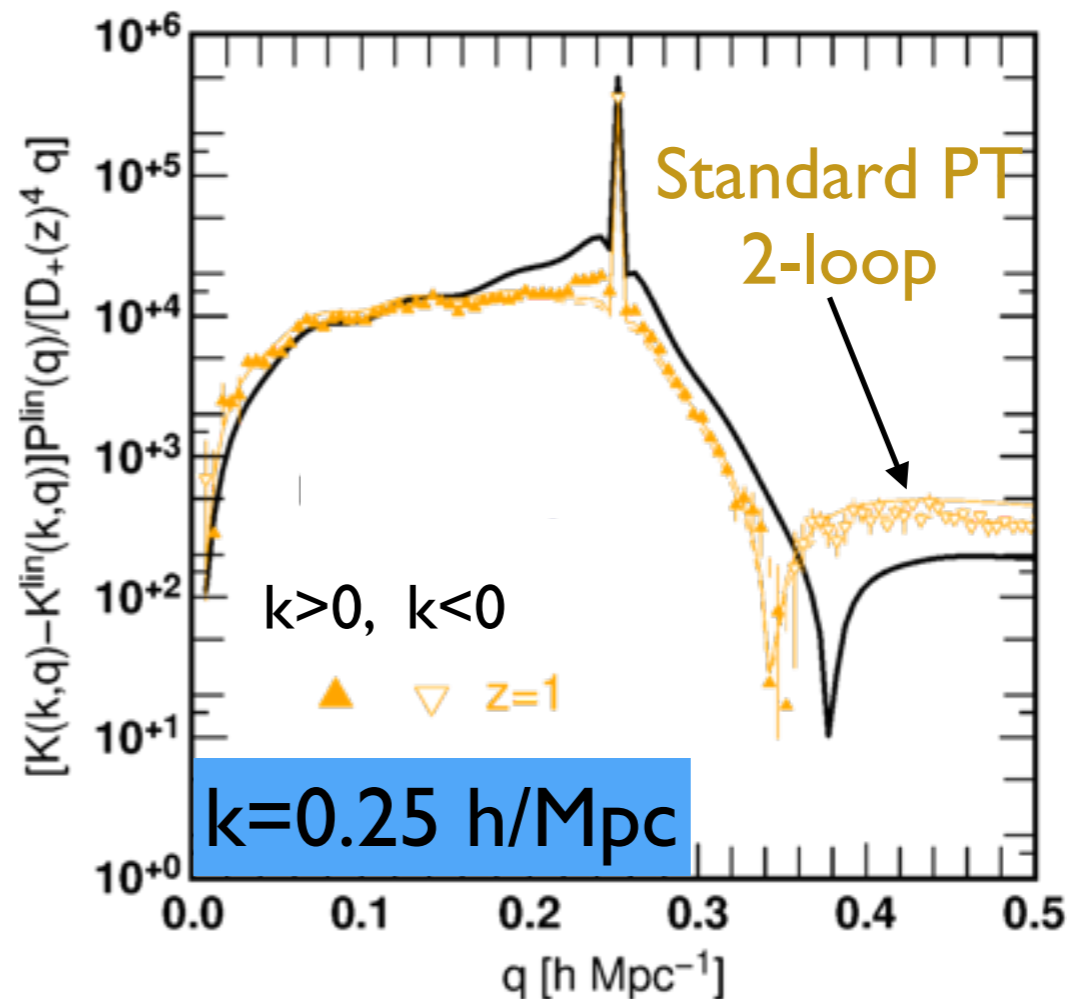
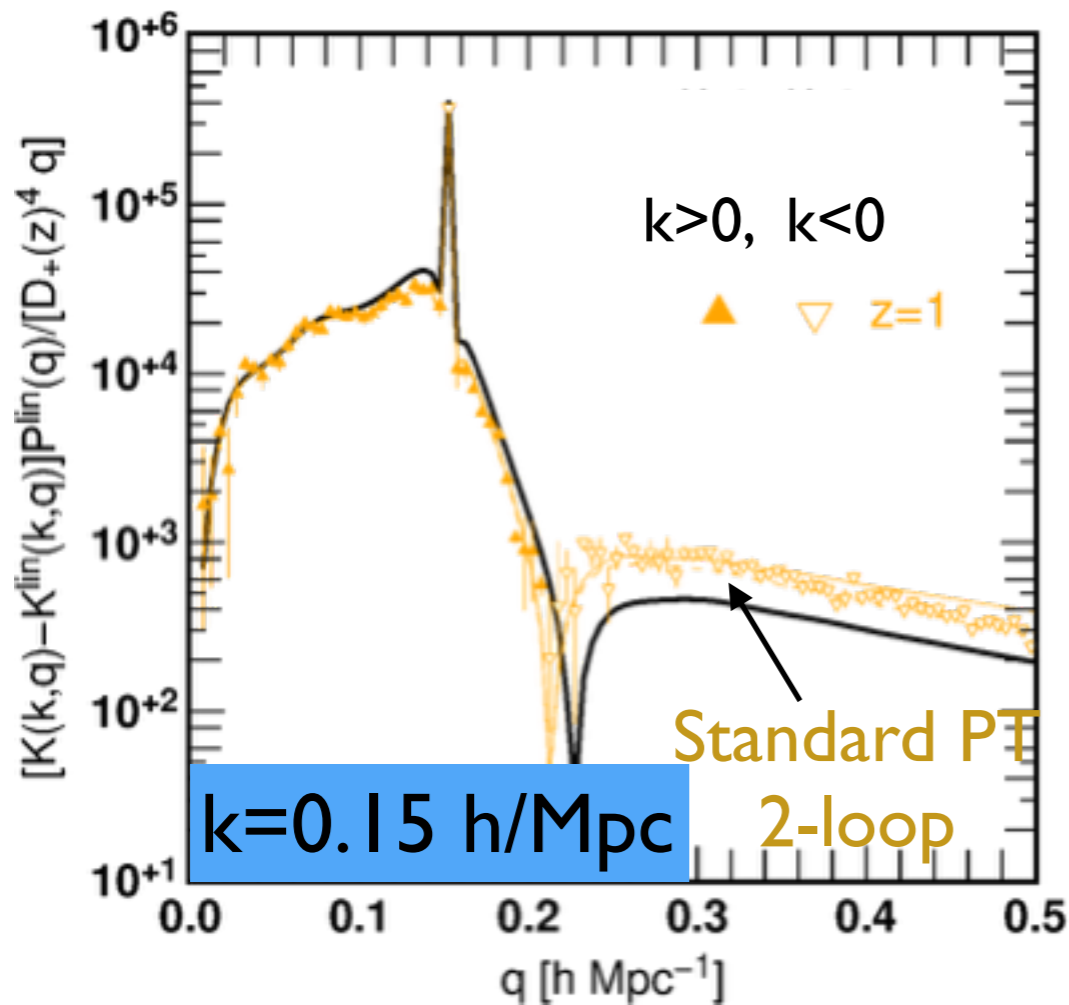


Discrepancy is manifest even at the scales (k) where the superficial agreement with simulation was found

Testing EFT approach (1-loop)

Response function
of $P(k)$

$$K(k, q) = q \frac{\delta P_{\text{nl}}(k)}{\delta P_0(q)}$$



$10^{-7} c^2$
 $2 \times 10^{-7} c^2$

Rather than EFT corrections, 2-loop corrections of standard PT give a much better result (although disagree at $k > 1 \text{ h/Mpc}$)

Vlasov-Poisson: back to the source

My personal viewpoint

- EFT is far more than complete treatment
- No more than the revival of the old debates
(e.g., Adhesion model by Gurvator et al. '89)

To understand what is going on,
we have to go back to a more fundamental treatment :

**Vlasov-Poisson
system**

$$\left[a \frac{\partial}{\partial t} + \frac{\mathbf{v}}{a} \cdot \frac{\partial}{\partial \mathbf{x}} - a \frac{\partial \phi}{\partial \mathbf{x}} \cdot \frac{\partial}{\partial \mathbf{v}} \right] f(\mathbf{x}, \mathbf{v}; t) = 0$$

$$\nabla^2 \phi(\mathbf{x}; t) = 4\pi G a^2 \int d^3 \mathbf{v} f(\mathbf{x}, \mathbf{v}; t)$$

Vlasov-Poisson system

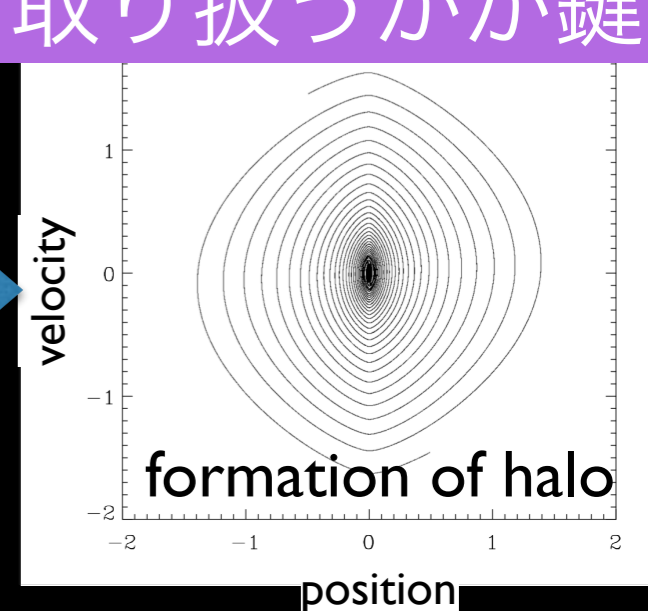
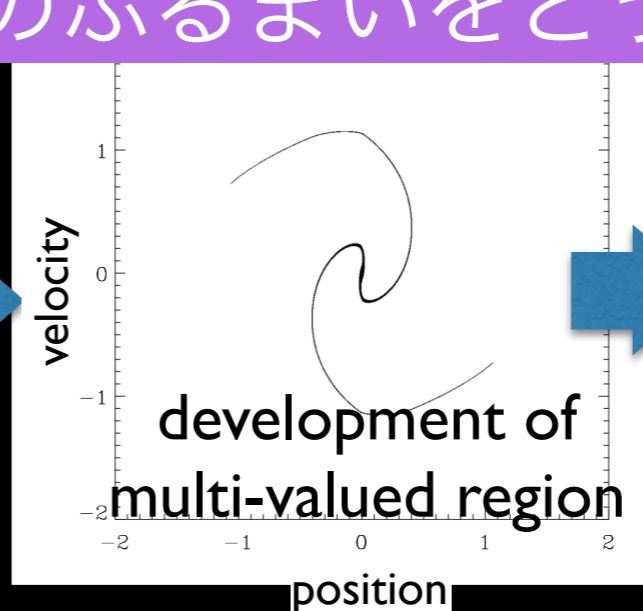
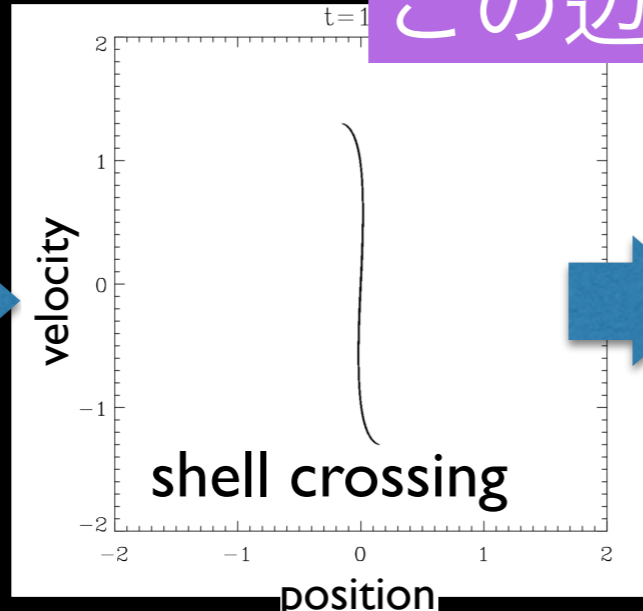
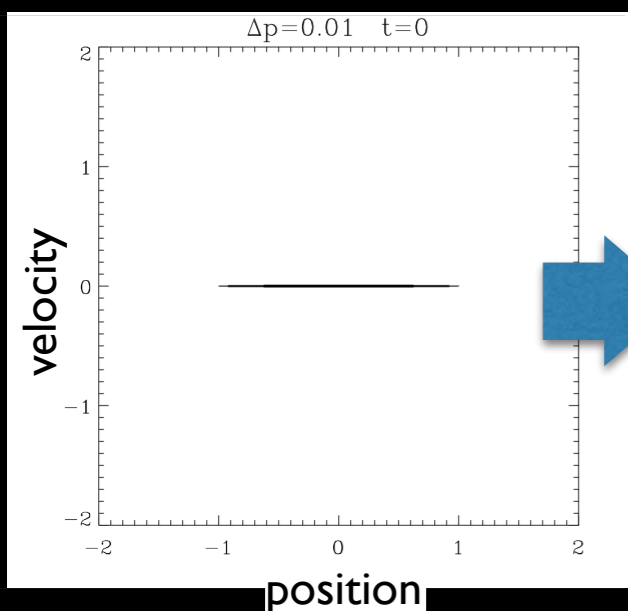
- $N \rightarrow \infty$ limit of self-gravitating N-body system (assuming that particles are not correlated with each other)
- Can be reduced to a pressureless fluid system if we assume single-stream flow:

$$f(\mathbf{x}, \mathbf{v}; t) \rightarrow \bar{\rho}(t) \{1 + \delta(\mathbf{x}; t)\} \delta_{\mathbf{D}}(\mathbf{v} - \mathbf{v}(\mathbf{x}; t))$$

But, single-stream flow is violated at small scales

Example: 1D collapse

この辺のふるまいをどう取り扱うかが鍵



Development of 6D Vlasov code

THE ASTROPHYSICAL JOURNAL, 762:116 (18pp), 2013 January 10

© 2013. The American Astronomical Society. All rights reserved. Printed in the U.S.A.

doi:10.1088/0004-637X/762/2/116

2013年

6次元 (64^6)

DIRECT INTEGRATION OF THE COLLISIONLESS BOLTZMANN EQUATION IN SIX-DIMENSIONAL PHASE SPACE: SELF-GRAVITATING SYSTEMS

KOHI YOSHIKAWA¹, NAOKI YOSHIDA^{2,3}, AND MASAYUKI UMEMURA¹

¹ Center for Computational Sciences, University of Tsukuba, 1-1-1 Tennodai, Tsukuba, Ibaraki 305-8577, Japan; kohji@ccs.tsukuba.ac.jp

² Department of Physics, The University of Tokyo, Tokyo 113-0033, Japan

³ Kavli Institute for the Physics and Mathematics of the Universe, The University of Tokyo, Kashiwa, Chiba 277-8583, Japan

Received 2012 June 18; accepted 2012 November 23; published 2012 December 20

An adaptively refined phase-space element method for cosmological simulations and collisionless dynamics

Oliver Hahn^{*1} and Raul E. Angulo^{†2}

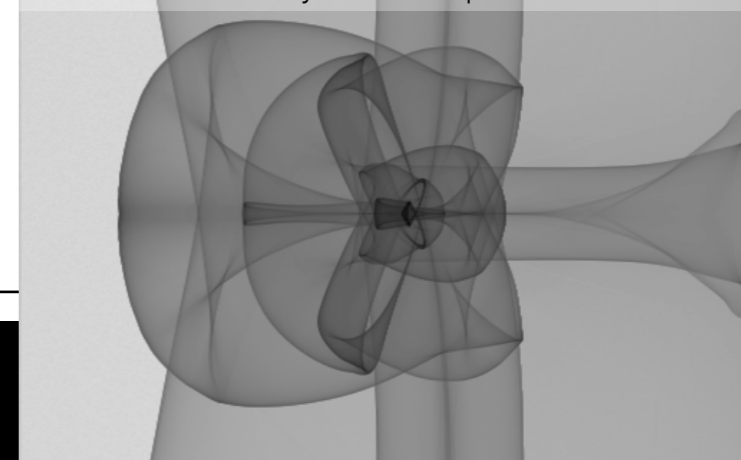
¹ Department of Physics, ETH Zurich, CH-8093 Zürich, Switzerland

² Centro de Estudios de Física del Cosmos de Aragón, Plaza San Juan 1, Planta-2, 44001, Teruel, Spain.

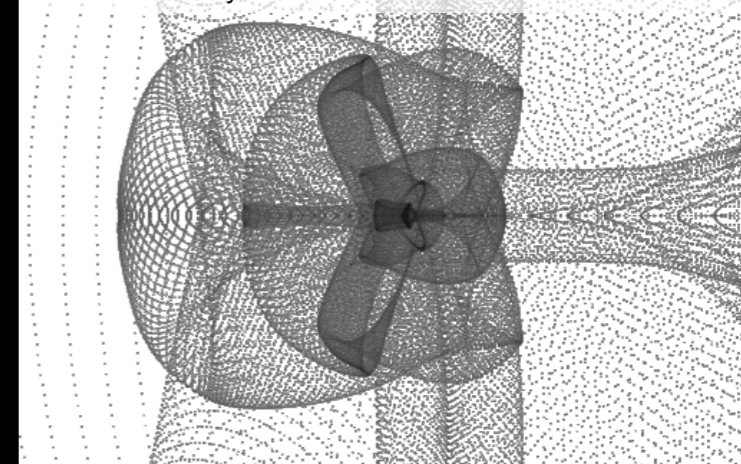
submitted to MNRAS Jan. 8, 2015

2015年

b. 32^3 + two level dynamic adaptive refinement



c. 512^3 N-body

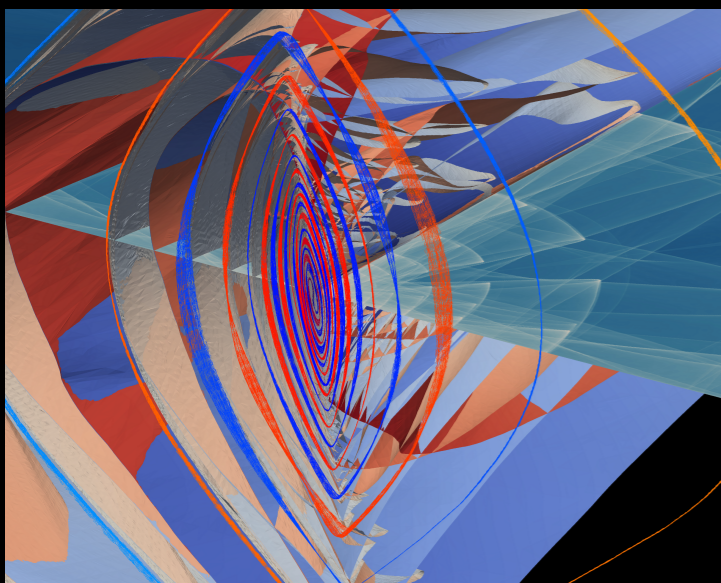


A phase-space Vlasov-Poisson solver for cold dark matter

Thierry Sousbie and Stephane Colombi

Institut D'Astrophysique de Paris, CNRS UMR 7095 and UPMC, 98bis, bd. Arago, F-75014, Paris, France

2015年 in prep.

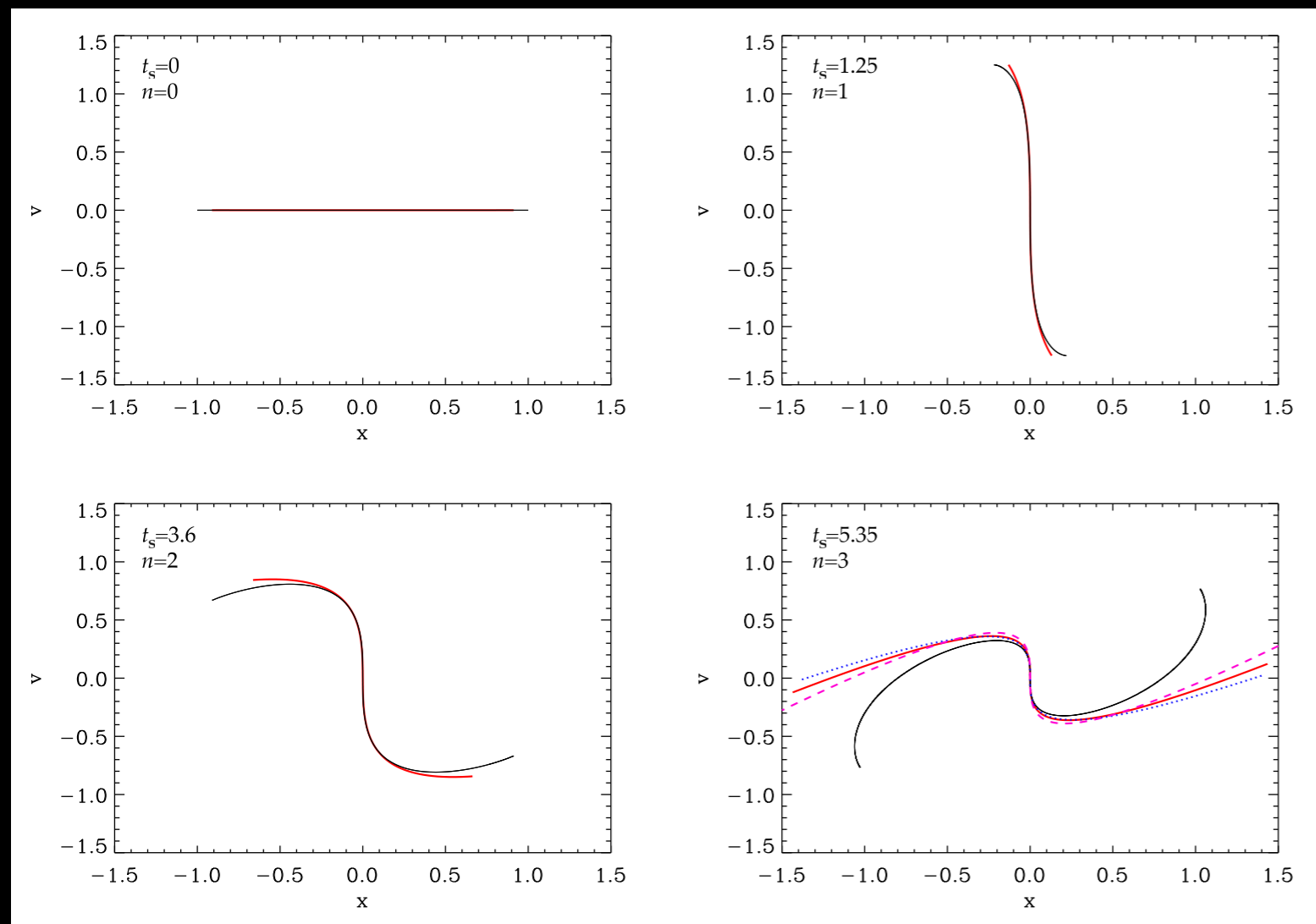


Post-collapse perturbation theory

Not only numerical technique, but also analytical technique to treat Vlasov system should be developed (especially for cold case)

An attempt has been made very recently in simple 1D collapse case

Colombi ('15)



Extension / generalization to cosmological case (1D & 3D) need to be developed

AT, Colombi, ... in progress

Summary

Development of theoretical calculation of large-scale structure as a fundamental cosmological tool in the light of precision cosmology

Success ----- Development of improved PT based on propagators

- ✓ resummed PT with multi-point propagators
- ✓ Fast calculation at 2-loop order

Limitation ----- Curse of UV divergence in PT calculation

& Beyond

- ✓ need effective field theory to cure this ? *Probably no !*
- ✓ need new treatment based on Vlasov-Poisson *in progress*

A deep investigation of PT is still necessary, but it will give a great impact on future cosmological science with LSS